

Phase-space entropy cascade and irreversibility of stochastic heating in nearly collisionless plasma turbulence

Michael L. Nastac,^{1,2,3,*} Robert J. Ewart,^{1,4} Wrick Sengupta,^{5,6}
Alexander A. Schekochihin,^{1,7} Michael Barnes,^{1,8} and William D. Dorland^{1,3,9}

¹*Rudolf Peierls Centre for Theoretical Physics, University of Oxford,
Clarendon Laboratory, Parks Road, Oxford OX1 3PU, UK*

²*St. John's College, Oxford OX1 3JP, UK*

³*Institute for Research in Electronics and Applied Physics,
University of Maryland, College Park, MD, 20742, USA*

⁴*Balliol College, Oxford, OX1 3BJ, UK*

⁵*Department of Astrophysical Sciences, Princeton University, Princeton, New Jersey 08543, USA*

⁶*Princeton Plasma Physics Laboratory, Princeton, New Jersey 08540, USA*

⁷*Merton College, Oxford OX1 4JD, UK*

⁸*University College, Oxford OX1 4BH, UK*

⁹*Department of Physics, University of Maryland, College Park, Maryland 20740, USA*

(Dated: June 17, 2024)

We consider a nearly collisionless plasma consisting of a species of ‘test particles’ in one spatial and one velocity dimension, stirred by an externally imposed stochastic electric field—a kinetic analogue of the Kraichnan model of passive advection. The mean effect on the particle distribution function is turbulent diffusion in velocity space—known as stochastic heating. Accompanying this heating is the generation of fine-scale structure in the distribution function, which we characterize with the collisionless (Casimir) invariant $C_2 \propto \iint dx dv \langle f^2 \rangle$ —a quantity that here plays the role of (negative) entropy of the distribution function. We find that C_2 is transferred from large scales to small scales in both position and velocity space via a phase-space cascade enabled by both particle streaming and nonlinear interactions between particles and the stochastic electric field. We compute the steady-state fluxes and spectrum of C_2 in Fourier space, with k and s denoting spatial and velocity wavenumbers, respectively. In our model, the nonlinearity in the evolution equation for the spectrum turns into a fractional Laplacian operator in k space, leading to anomalous diffusion. Whereas even the linear phase mixing alone would lead to a constant flux of C_2 to high s (towards the collisional dissipation range) at every k , the nonlinearity accelerates this cascade by intertwining velocity and position space so that the flux of C_2 is to both high k and high s simultaneously. Integrating over velocity (spatial) wavenumbers, the k -space (s -space) flux of C_2 is constant down to a dissipation length (velocity) scale that tends to zero as the collision frequency does, even though the rate of collisional dissipation remains finite. The resulting spectrum in the inertial range is a self-similar function in the (k, s) plane, with power-law asymptotics at large k and s . Our model is fully analytically solvable, but the asymptotic scalings of the spectrum can also be found via a simple phenomenological theory whose key assumption is that the cascade is governed by a ‘critical balance’ in phase space between the linear and nonlinear time scales. We argue that stochastic heating is made irreversible by this entropy cascade and that, while collisional dissipation accessed via phase mixing occurs only at small spatial scales rather than at every scale as it would in a linear system, the cascade makes phase mixing even more effective overall in the nonlinear regime than in the linear one.

I. INTRODUCTION

Understanding the nature of turbulent cascades in nearly collisionless space and astrophysical plasmas is an outstanding problem [1–7] with a diverse range of applications, from solving the coronal-heating problem [7] to interpreting radiation emission from accretion disks around black holes [8–10]. A major difficulty distinguishing such turbulence from its fluid counterparts lies in the fact that fluctuations evolve in the six-dimensional phase space of single-particle positions and velocities. Dissipation (in the sense of irreversible entropy production)

occurs via particle collisions [11, 12], which in a nearly collisionless plasma are activated only when the particle distribution function develops large gradients in velocity space.

Turbulent dissipation in nearly collisionless plasmas is often considered from an energetics perspective. This point of view focuses on the cascade of bulk kinetic and electromagnetic energy from large to small spatial scales (see, e.g., [4, 13–16] and references therein) and the physical processes, such as magnetic reconnection [17–20] and wave-particle interactions [1, 6], that convert this energy into the internal energy of the plasma. Whilst energy-cascade and transfer mechanisms are important, they provide a fundamentally incomplete picture of turbulent dissipation. Without collisions, entropy is formally conserved (along with an infinity of Casimir invariants [21]),

* michael.nastac@physics.ox.ac.uk

and any transfer of energy between particles and fields is formally reversible.

It was realized by [22, 23] that entropy production in the long-time limit of a nearly collisionless plasma must remain finite even as the collision frequency ν tends to zero. This idea crystallized in [2, 24–26], where the notion of entropy cascade in the context of gyrokinetics was introduced. Below the Larmor scale, in a phase-space inertial range between the injection range at large scales and the collisional dissipation range at small scales, the (negative) entropy of the perturbed distribution function cascades in both position and velocity space via a nonlinear perpendicular phase-mixing mechanism [27]. Because this is a constant-flux cascade, the turbulent heating rate in a gyrokinetic plasma is finite and independent of ν even as $\nu \rightarrow 0^+$, analogous to so-called dissipative anomalies [28, 29] in hydrodynamics, where viscous dissipation is finite in infinite-Reynolds-number turbulence.

Entropy cascade outside the gyrokinetic approximation is a frontier topic just beginning to be explored [30–34]. In this paper, we study turbulent dissipation and entropy cascade via an analytically solvable model introduced by [35]. We consider the ‘1D-1V’ electrostatic, full- f Vlasov equation with a model diffusive collision operator for a test-particle species, where instead of the electric field being self-consistently determined by Poisson’s equation, it is externally determined to be a stochastic Gaussian, white-noise source with a specified spatial correlation function. Physically, this model represents the evolution of a low-density minority species in a multi-component plasma whose dielectric response is dominated by the other, more abundant species. This model is the plasma-kinetic analogue of the Kraichnan [36] model of passive advection, where a scalar field [37], such as temperature or concentration of dye, is passively advected by an externally determined random flow, allowing for analytical calculations of the passive-scalar statistics. The Kraichnan model has been dubbed the ‘Ising model’ [38] of fluid turbulence because it is a solvable model that exhibits many properties also present in real systems, and so serves as a theoretical laboratory to study turbulence [39]. It is in this spirit that we investigate our solvable model of kinetic plasma turbulence.

We decompose the distribution function into its mean and fluctuating parts, $f = \langle f \rangle + \delta f$, where $\langle \dots \rangle$ denotes ensemble averaging over realizations of the random electric field. In our model, particles are stochastically accelerated by the electric field and undergo random walks in velocity space, resulting in bulk heating of $\langle f \rangle$ [40]. In the context of magnetized plasmas, this phenomenon is often referred to as stochastic heating [6, 41, 42]. Accompanying this heating is the generation of velocity and spatial structure in the perturbed distribution function δf via linear phase mixing and nonlinear interactions between particles and the turbulent electric field [35].

We characterize this structure via the collisionless (Casimir) invariant $C_2 = (1/L) \iint dx dv \langle f^2 \rangle / 2$, where L is the system size. C_2 has been considered before as a

measure of phase-space structure and as a cascaded quantity in kinetic plasma turbulence [30, 32, 35, 43–47], and is closely related to the part of the traditional entropy, $S = - \iint dx dv f \log f$, associated with the perturbed distribution function and entering additively in the free-energy invariant of δf gyrokinetics [2, 22, 24, 48, 49]. The conservation of C_2 is broken by particle collisions, and, in particular, when collisions are modeled as a linear diffusion operator in velocity space, as they are in this paper, the collisional dissipation of C_2 is negative-definite. Because the time irreversibility of our system can be tracked via non-conservation of C_2 , it can be used as a generalized (negative) entropy of the distribution function.

The diffusion of $\langle f \rangle$ by the electric field has the side effect of injecting $\delta C_2 = (1/L) \iint dx dv \langle \delta f^2 \rangle / 2$ fluctuations at large scales. These are then cascaded to small scales in both position and velocity space, where they are ultimately dissipated by collisions. This phase-space cascade of δC_2 is due to both linear phase mixing and nonlinear interactions between particles and the stochastic electric field. We analyze this cascade by computing the steady-state Fourier spectrum and fluxes of δC_2 in both position and velocity space, with dual variables (wavenumbers) k and s , respectively.

In the absence of nonlinearity, linear phase mixing advects the spectrum from low to high $|s|$, giving rise to an ‘inertial range’ in s where there is a constant flux of δC_2 from injection to dissipation scales, at every k [50, 51]. The resulting steady-state spectrum is flat in the inertial range, with an exponential cutoff at a ν -dependent collisional scale s_ν .

Under the Kraichnan model, we find that the nonlinear term in the evolution equation for the Fourier spectrum becomes a fractional Laplacian operator [52–54] in k space, which leads to anomalous diffusion [55, 56]. Whereas fractional Laplacians (and fractional derivatives in general) are usually introduced in an ad-hoc manner to model systems with anomalous diffusion, both in plasma physics [57–59] and a wide variety of other contexts [60], here it emerges naturally as a result of our assumptions about the electric field.

The linear phase mixing and the turbulent fractional diffusion intertwine the position- and velocity-space cascades in such a way that the resulting spectrum is a self-similar function in the (k, s) plane, with power-law asymptotics at large k and s . Even though the Kraichnan model is fully analytically solvable, we can also recover these asymptotic scalings via a phenomenological theory whose key assumption is that the cascade is governed by a ‘critical balance’ in phase space between the linear and nonlinear time scales.

The δC_2 flux has components in both k and s directions. The flow of δC_2 occurs along outward unwinding spirals in (k, s) space. This circuitous route to dissipation scales is due to the nonlinearity generating modes that can linearly propagate from high to low $|s|$, called ‘phase-unmixing’ modes [61], a stochastic generalization

of the textbook phenomenon of plasma echo [62, 63]. The net result after adding together contributions to the flux from the phase-mixing and phase-unmixing modes is that δC_2 is cascaded to both high s and high k simultaneously, and collisional dissipation only occurs at scales comparable to, or smaller than, the dissipation length and velocity scales, both of which tend to zero when the collision frequency ν does. Integrating over velocity (spatial) wavenumbers, the flux of δC_2 in k (s) space is constant down to these dissipation scales, beyond which perturbations are thermalized by collisions. The rate of collisional dissipation is finite and independent of the collision frequency as $\nu \rightarrow 0^+$ —a clear analytical example of a ‘dissipative anomaly’ in a kinetic system. This turbulent dissipation ultimately mediates the irreversibility of the stochastic heating.

The rest of this paper is organized as follows. In Section II, we introduce the Vlasov-Kraichnan model. In Section III, we construct a phenomenological theory that captures the asymptotic scalings of the Fourier spectrum of δC_2 . Then, in Section IV, we directly calculate the 1-D phase-space fluxes of δC_2 in Fourier space in a statistical steady state. In Section V, we calculate the inertial-range Fourier spectrum and its corresponding 2-D fluxes in (k, s) space. Finally, in Section VI, we conclude our results and discuss their implications. Supplementary calculations and discussions are exiled to Appendices A-E.

II. KRAICHNAN MODEL FOR A 1D-1V ELECTROSTATIC PLASMA

We consider a test-particle species composed of particles with charge q and mass m in a 1D periodic box of length L , and subject to an external electric field E . At $t = 0$, we assume the particle distribution function f to have no spatial variation, but we keep its velocity dependence generic, only assuming that f is square-integrable and has finite kinetic energy. We denote the number density of the distribution function as n_0 and the initial thermal velocity as $v_{\text{th},0} = \sqrt{2T_0/m}$, where T_0 is the initial temperature of the particles. An example initial condition with these properties is a Maxwellian,

$$f(x, v, t = 0) = \frac{n_0}{\sqrt{\pi}v_{\text{th},0}} e^{-v^2/v_{\text{th},0}^2} \equiv F_M(v). \quad (1)$$

The Vlasov equation for the particle distribution function is

$$\frac{\partial f}{\partial t} + v \frac{\partial f}{\partial x} + E \frac{\partial f}{\partial v} = C[f], \quad (2)$$

where $C[f]$ is the collision operator, and we have absorbed q and m into the definition of E , denoting $qE/m \rightarrow E$.

We assume E to be a Gaussian white-noise field, with zero mean and correlation function

$$\langle E(x, t)E(x', t') \rangle = 2D(x, x') \delta(t - t'), \quad (3)$$

where $\langle \dots \rangle$ denotes ensemble averaging over realizations of E and δ is a Dirac delta distribution. We assume E to be statistically homogeneous and isotropic in space, so $D(x, x') = D(r)$, where $r = |x - x'|$. We choose

$$D(r) = \sum_k e^{ikr} \hat{D}(k), \quad (4)$$

where $k \in (2\pi/L)\mathbb{Z}$ and

$$\hat{D}(k) = D \frac{e^{-(\eta k)^2}}{(k^2 + L_E^{-2})^{(\alpha+1)/2}}. \quad (5)$$

Here, D is a constant diffusion coefficient with dimensions $(\text{length}^{1-\alpha}) \times (\text{time}^{-3})$, $0 < \alpha \leq 2$, and L_E and η represent the integral length scale and dissipation scale, respectively, of the stochastic electric field.

The electric field is chosen so that its correlation function (3) has a power-law spectrum $\propto |k|^{-(\alpha+1)}$ in the inertial range $1/L_E \ll k \ll 1/\eta$; note that (5) is defined in a similar way to the velocity field in the fluid passive scalar Kraichnan model [39, 64]. We identify two distinct regimes: $\alpha < 2$ and $\alpha = 2$. When $\alpha < 2$, the field is multiscale, reminiscent of turbulent fields in fully developed turbulence. When $\alpha = 2$, the spectrum is sufficiently steep that the field is effectively single-scale. This case is known as the Batchelor regime [65]. While there are important differences between the two regimes [39], some of which we will discuss, many of the properties of the model considered in this paper will be qualitatively the same in both regimes.

It will be useful to decompose the distribution function into its mean and fluctuating parts:

$$f = \langle f \rangle + \delta f. \quad (6)$$

We make no assumption of δf being small compared to $\langle f \rangle$.

The effect of collisions will be to wipe out fine-scale velocity-space structure in the distribution function. To model this in the simplest possible way, we ignore collisions between our test-particle species and the other species in the plasma, and represent collisions within the test species as a linear diffusion in velocity space acting only on δf , viz.,

$$C[\delta f] = \nu \frac{\partial^2 \delta f}{\partial v^2}, \quad (7)$$

where ν is the collision frequency (multiplied by $v_{\text{th},0}^2$), which we consider to be vanishingly small, taking $\nu \rightarrow 0^+$. It is not a problem that (7) does not conserve energy or vanish on a Maxwellian because collisions will only matter for the parts of δf with sharp gradients in v [66].

A. Stochastic heating

We first work out the effect of the turbulent electric field on the mean distribution function. Ensemble averaging (2) over realizations of the stochastic electric field, we get

$$\frac{\partial \langle f \rangle}{\partial t} + v \frac{\partial \langle f \rangle}{\partial x} + \left\langle E \frac{\partial \delta f}{\partial v} \right\rangle = 0. \quad (8)$$

The equation for δf is then

$$\begin{aligned} \frac{\partial \delta f}{\partial t} + v \frac{\partial \delta f}{\partial x} + E \frac{\partial \delta f}{\partial v} - \left\langle E \frac{\partial \delta f}{\partial v} \right\rangle \\ = -E \frac{\partial \langle f \rangle}{\partial v} + \nu \frac{\partial^2 \delta f}{\partial v^2}. \end{aligned} \quad (9)$$

To compute the ensemble average of the nonlinear term in (8), we apply the Furutsu-Novikov theorem [67, 68] for splitting correlators. For a Gaussian field E that depends on variables \mathbf{q} , this theorem states that

$$\langle E(\mathbf{q}) F[E] \rangle = \int d\mathbf{q}' \langle E(\mathbf{q}) E(\mathbf{q}') \rangle \left\langle \frac{\delta F[E]}{\delta E(\mathbf{q}')} \right\rangle, \quad (10)$$

where $F[E]$ is a differentiable functional of E . Formally integrating (9) with respect to time, we have that

$$\begin{aligned} \delta f = - \int^t dt'' \left[v \frac{\partial \delta f}{\partial x} + E \frac{\partial \delta f}{\partial v} - \left\langle E \frac{\partial \delta f}{\partial v} \right\rangle \right. \\ \left. + E \frac{\partial \langle f \rangle}{\partial v} - \nu \frac{\partial^2 \delta f}{\partial v^2} \right](t''). \end{aligned} \quad (11)$$

Combining (10) and (11), we have

$$\begin{aligned} \langle E(x, t) \delta f(x, t) \rangle \\ = \int dt' \int dx' \langle E(x, t) E(x', t') \rangle \left\langle \frac{\delta [\delta f(x, t)]}{\delta E(x', t')} \right\rangle \\ = - \int dx' D(x - x') \delta(x - x') \frac{\partial \langle f \rangle}{\partial v} = -D(0) \frac{\partial \langle f \rangle}{\partial v}. \end{aligned} \quad (12)$$

Therefore, (8) becomes

$$\frac{\partial \langle f \rangle}{\partial t} = D_0 \frac{\partial^2 \langle f \rangle}{\partial v^2}, \quad (13)$$

where $D_0 = D(0)$ is the ‘turbulent collisionality.’ We have dropped the streaming term in (8) because our initial condition is spatially homogeneous, so $\langle f \rangle$ at future times does not depend on x . The solution to (13) is

$$\langle f \rangle = \int dv' f(v', t=0) \frac{1}{\sqrt{4\pi D_0 t}} e^{-(v-v')^2/4D_0 t}. \quad (14)$$

The mean kinetic-energy density $\langle K \rangle$ of this distribution function is

$$\langle K \rangle \equiv \int dv \frac{mv^2}{2} \langle f \rangle = K_0 + mn_0 D_0 t, \quad (15)$$

where K_0 is the initial kinetic-energy density. For the Maxwellian initial condition (1), (14) becomes simply

$$\langle f \rangle = \frac{n_0}{\sqrt{\pi} v_{\text{th}}} e^{-v^2/v_{\text{th}}^2}, \quad (16)$$

with a growing thermal speed:

$$v_{\text{th}} = \sqrt{v_{\text{th},0}^2 + 4D_0 t}. \quad (17)$$

As particles get stochastically accelerated by the electric field, they undergo Brownian random walks in velocity space, leading to bulk heating of the distribution function [40], with secularly growing kinetic energy (15). In magnetized plasmas, this phenomenon is usually referred to as stochastic heating [6, 41, 42].

B. C_2 budget: injection and dissipation

Because the stochastic electric field continuously heats the distribution function, viz., (15), energy is not a conserved quantity in our system. However, what is conserved in the absence of collisions is the quadratic quantity

$$C_2 = \frac{1}{L} \iint dx dv \frac{1}{2} \langle f^2 \rangle = C_{2,0} + \delta C_2, \quad (18)$$

where

$$C_{2,0} = \frac{1}{L} \iint dx dv \frac{1}{2} \langle f \rangle^2, \quad (19)$$

$$\delta C_2 = \frac{1}{L} \iint dx dv \frac{1}{2} \langle \delta f^2 \rangle. \quad (20)$$

C_2 can only change via collisions. Using (2) and (7), we have

$$\begin{aligned} \frac{dC_2}{dt} &= \frac{1}{L} \iint dx dv \langle \delta f C[\delta f] \rangle \\ &= -\frac{\nu}{L} \iint dx dv \left\langle \left| \frac{\partial \delta f}{\partial v} \right|^2 \right\rangle. \end{aligned} \quad (21)$$

Thus, when collisions are approximated as a linear diffusion in velocity space, they provide negative-definite dissipation of C_2 . Because $-C_2$ is conserved in the absence of collisions and positive-definitely increased by collisions, we can interpret it as a ‘generalized entropy’ of the distribution function. We will henceforth refer to $-C_2$ and entropy synonymously.

Stochastic heating, which is a collisionless process, is accompanied by the decrease of $C_{2,0}$. Indeed, using (13) and integrating by parts, we have

$$\begin{aligned} \frac{dC_{2,0}}{dt} &= -\frac{D_0}{L} \iint dx dv \left| \frac{\partial \langle f \rangle}{\partial v} \right|^2 \\ &= -D_0 \int dv \left| \frac{\partial \langle f \rangle}{\partial v} \right|^2 \leq 0 \end{aligned} \quad (22)$$

generically, and for a Maxwellian in particular,

$$\frac{dC_{2,0}}{dt} = -\frac{n_0^2 \sqrt{m}}{8\sqrt{\pi}} \frac{1}{T^{3/2}} \frac{dT}{dt}, \quad (23)$$

where $T = mv_{\text{th}}^2/2$, with v_{th} given by (17). To work out the δC_2 budget, we can combine (18) and (21), giving

$$\frac{d\delta C_2}{dt} = D_0 \int dv \left| \frac{\partial \langle f \rangle}{\partial v} \right|^2 - \frac{\nu}{L} \iint dx dv \left\langle \left| \frac{\partial \delta f}{\partial v} \right|^2 \right\rangle. \quad (24)$$

Thus, without collisions, as $C_{2,0}$ decreases as a result of the stochastic heating of $\langle f \rangle$, δC_2 increases to maintain entropy balance. Once δf has developed sharp enough gradients, collisions dissipate δf , increasing the total entropy. The irreversibility of stochastic heating therefore hinges on the collisional dissipation of δf .

If the δC_2 fluctuations evolve faster than the mean $C_{2,0}$ and reach a quasi-steady state (as we shall argue that they do), then (24) becomes

$$D_0 \int dv \left| \frac{\partial \langle f \rangle}{\partial v} \right|^2 = \frac{\nu}{L} \iint dx dv \left\langle \left| \frac{\partial \delta f}{\partial v} \right|^2 \right\rangle. \quad (25)$$

In the case where the initial condition is Maxwellian, combining (23) and (22) and substituting this expression into (25) yields a direct balance between the heating rate of $\langle f \rangle$ and the collisional dissipation of δf .

The velocity-space gradients of $\langle f \rangle$ inject δC_2 at large scales, and collisions dissipate δC_2 at small scales. As in any prototypical turbulent system, the steady-state balance (25) between injection and dissipation at such disparate scales can hold if there is a constant-flux cascade bridging them. This is precisely what we will find in the following sections, viz., a phase-space cascade of δC_2 in both position and velocity space. This cascade will be our focus for the rest of this paper.

Before continuing, we note that in Appendix A, we discuss alternative formulations of the thermodynamics of our system in terms of other collisionless invariants, and why in this work we have chosen to study C_2 over those other invariants.

C. Evolution of Fourier spectrum

We analyze how δC_2 is partitioned between scales in phase space via its Fourier spectrum. We define

$$\delta \hat{f}(k, s) = \frac{1}{2\pi L} \iint dx dv e^{-i(kx-sv)} \delta f(x, v), \quad (26)$$

$$\langle \hat{f} \rangle(s) = \frac{1}{2\pi} \int dv e^{isv} \langle f \rangle(v), \quad (27)$$

and

$$\hat{E}(k) = \frac{1}{L} \int dx e^{-ikx} E(x), \quad (28)$$

where k and s are dual variables to x and v , respectively. Fourier transforming (9), we get that $\delta \hat{f}(k, s)$ satisfies

$$\begin{aligned} \frac{\partial \delta \hat{f}}{\partial t} + k \frac{\partial \delta \hat{f}}{\partial s} \\ - is \sum_p \left[\hat{E}(p) \delta \hat{f}(k-p) - \langle \hat{E}(p) \delta \hat{f}(k-p) \rangle \right] \\ = is \hat{E} \langle \hat{f} \rangle - \nu s^2 \delta \hat{f}. \end{aligned} \quad (29)$$

We define the Fourier spectrum as

$$\hat{F}(k, s) = \frac{1}{2} \langle |\delta \hat{f}(k, s)|^2 \rangle, \quad (30)$$

which satisfies Parseval's theorem,

$$\delta C_2 = \frac{1}{L} \iint dx dv \frac{1}{2} \langle \delta f^2 \rangle = 2\pi \sum_k \int ds \hat{F}(k, s), \quad (31)$$

has the budget equation (equivalent to (24) in spectral space)

$$\frac{d\delta C_2}{dt} = 2\pi \left[\sum_k \int ds \hat{S} - 2\nu \sum_k \int ds s^2 \hat{F} \right], \quad (32)$$

and satisfies the evolution equation

$$\frac{\partial \hat{F}}{\partial t} + k \frac{\partial \hat{F}}{\partial s} + \kappa s^2 (-\Delta_k)^{\alpha/2} \hat{F} = \hat{S} - 2\nu s^2 \hat{F}. \quad (33)$$

Equation (33) is important, and its analysis will be the focus of the rest of this paper. There are several steps required to derive (32) and (33) from (29), primarily using (10) to calculate correlation functions involving the electric field. These steps are technical, so we detail them in Appendix B.

The source term in (32) and (33) is

$$\hat{S}(k, s) = \hat{D}(k) s^2 \langle \hat{f} \rangle^2, \quad (34)$$

which for a Maxwellian initial condition evaluates to

$$\hat{S}(k, s) = \frac{n_0^2}{(2\pi)^2} \hat{D}(k) s^2 e^{-s^2 v_{\text{th}}^2/2}, \quad (35)$$

where v_{th} is given by (17).

In (33), $(-\Delta_k)^{\alpha/2}$ is a fractional Laplacian [52–54] of order $\alpha/2$ (in k space), and κ is a turbulent diffusion coefficient $\propto LD$, for which the exact expression is given in Appendix B. To obtain this term, we have taken the limit $\eta \rightarrow 0^+$ in (5), which is analogous to taking the zero-viscosity limit in hydrodynamic turbulence, and $kL_E \gg 1$, which is a convenient limit to take to focus on how the distribution function is stirred in the ‘inertial range’ of the stochastic electric field.

The fractional Laplacian is a non-local integral operator, generalizing the Laplacian to non-integer order. Its Fourier transform satisfies

$$\frac{L}{2\pi} \int dk e^{ikr} (-\Delta_k)^{\alpha/2} \hat{F}(k, s) = |r|^\alpha F(r, s), \quad (36)$$

where

$$F(r, s) = \frac{L}{2\pi} \int dk e^{ikr} \hat{F}(k, s). \quad (37)$$

Note that we have converted sums over k into integrals (multiplied by the inverse step size $L/2\pi$).

Mathematically, the fractional Laplacian describes abstract ‘particles’ with coordinates (k, s) undergoing random jumps in k space, so-called Lévy flights, which leads to superdiffusion [55, 56]. In the limit $\alpha \rightarrow 2^-$, the fractional Laplacian becomes (minus) a regular Laplacian [52], corresponding to regular Brownian motion. This limit, the Batchelor regime, was studied before in [35], although we shall present some new conclusions about it below.

In the following sections, we will solve for steady-state solutions of (33). To this end, we further assume that the source is localized at small (k, s) and injects δC_2 at a constant rate,

$$L \iint dk ds \hat{S}(k, s) = \varepsilon > 0. \quad (38)$$

These assumptions may appear questionable in view of (24) and (22) (is the source really constant in time?) and of (34) and (5) (is it really local?). Before continuing, we address these concerns.

Regarding the constancy of the source, we observe that in (24), the injection rate of δC_2 via the stochastic heating of $\langle f \rangle$, using (22) and dimensional analysis, scales as

$$\varepsilon = -\frac{dC_{2,0}}{dt} \propto \frac{D_0 n_0^2}{v_{\text{th}}^3} = \frac{D_0 n_0^2}{(v_{\text{th},0}^2 + 4D_0 t)^{3/2}}. \quad (39)$$

This scaling is particularly obvious, from (23), for the case of a Maxwellian initial condition. Comparing (39) and (38), we see that the injection rate is, in fact, time-dependent, $\propto t^{-3/2}$, even though in our calculations we would like to treat ε as a constant. However, if the cascade of δC_2 is set up quickly compared to the decay of the source (which, as will be discussed in Section VI B, it is on a ν -independent time scale when $\alpha < 2$ and a time scale $\propto |\log \nu|$ when $\alpha = 2$), it is reasonable to treat the source as approximately constant on the time scale of the δf evolution, and then solve for the steady-state spectrum. This becomes an ever-better approximation at long times, because the rate of change of (39) is a decreasing function of time. Also note that, as long as $\varepsilon > 0$, its actual value is not important; because the spectrum-evolution equation (B8) is linear, it has no special amplitude scale, and so the size of ε is just a global modifier of the spectrum’s amplitude.

Regarding the locality of the source, it is easily satisfied in s space, as the velocity derivatives of $\langle f \rangle$ become ever smaller over time as the distribution function stochastically heats. This is clearly seen in the case of a Maxwellian initial condition, where the source (35) is a Gaussian in s , with a width $\sim 1/v_{\text{th}}$. In k space, the

source is not, in fact, truly localized, since $\hat{D}(k)$ is a power law, viz., (5), so fluctuations are injected at all scales where the electric field exists. However, this turns out not to be fatal to our formalism: we will neglect the source in our solving for the inertial-range spectrum in Sections III and V and argue *a posteriori* in Section V B that this choice was justified.

III. PHENOMENOLOGICAL THEORY OF PHASE-SPACE CASCADE

In Sections IV and V, we perform a detailed analysis of (33). However, the key results of those sections can, in fact, be intuited via a much simpler route, which we follow here first.

As discussed in Section II B, stochastic heating can only truly be made irreversible by particle collisions. For collisions to be relevant even in the limit $\nu \rightarrow 0^+$, we conjecture that δC_2 undergoes a cascade in both position and velocity space. Analogously to phenomenological theories of hydrodynamic turbulence [28, 69], we assume that there exists an inertial range in phase space, whereby the flux ε is processed between scales, from the injection to dissipation range. Under this assumption, our task is then to ascertain the form of the spectrum \hat{F} in (k, s) space in the inertial range.

Fluctuations of δf develop fine-scale structure in velocity space via linear phase mixing, which manifests in (33) as advection of \hat{F} in s at the rate k . Dimensionally, the phase-mixing time is, therefore,

$$\tau_p \sim \frac{s}{k}. \quad (40)$$

Likewise, δf develops fine-scale structure in position space via nonlinear mixing by the stochastic electric field, which manifests in (33) as fractional diffusion of \hat{F} in k with the diffusion coefficient κs^2 . Dimensionally, using (36), the turbulent-diffusion time is, therefore,

$$\tau_d \sim \frac{k^\alpha}{\kappa s^2}. \quad (41)$$

The ratio of these time scales (taken to the power $1/(\alpha + 1)$ for analytical convenience and in anticipation of the results of Section V) is

$$\xi = \left(\frac{\tau_d}{\tau_p} \right)^{1/(\alpha+1)} = \frac{k}{(\kappa s^3)^{1/(\alpha+1)}}. \quad (42)$$

We conjecture that the structure of \hat{F} in (k, s) space is governed by the parameter ξ . In particular, we assume that the spectrum is a product of power laws in k and s , with different scaling exponents depending on whether ξ is small or large:

$$\hat{F}(k, s) \propto \begin{cases} k^a s^{-b}, & \xi \ll 1, \\ k^{-c} s^d, & \xi \gg 1. \end{cases} \quad (43)$$

When $\xi \ll 1$, the turbulent-diffusion time is much shorter than the phase-mixing time, so we expect the inertial-range spectrum to satisfy, to lowest order in ξ ,

$$\kappa s^2 (-\Delta_k)^{\alpha/2} \hat{F} = 0, \quad (44)$$

and therefore, to be independent of k . Consequently, $a = 0$ in (43).

When $\xi \gg 1$, the phase-mixing time is much shorter than the turbulent-diffusion time. Then, to lowest order in $1/\xi$, we expect the spectrum to satisfy

$$k \frac{\partial \hat{F}}{\partial s} = 0, \quad (45)$$

and, therefore, to be independent of s , the same as in the linear regime [50, 51]. Consequently, $d = 0$ in (43).

To find b and c , we invoke our initial assumption of a constant-flux cascade. As in any Kolmogorov-style theory, we need a prescription for the cascade time τ_c , which is the typical time for δC_2 to be transferred across phase-space scales (ℓ, u) , where $\ell \sim 1/k$ and $u \sim 1/s$. We conjecture that the cascade time is set by the phase-mixing and turbulent-diffusion time scales (40) and (41), and that the latter two must balance along the path of the cascade:

$$\begin{aligned} \tau_c &\sim \tau_p \sim \tau_d \\ \implies \tau_c &\sim \kappa^{-1/3} \ell^{(2-\alpha)/3} \sim \kappa^{-1/(\alpha+1)} u^{(2-\alpha)/(\alpha+1)}. \end{aligned} \quad (46)$$

In wavenumber space, this condition is satisfied when $\xi \sim 1$, i.e.,

$$s \sim \kappa^{-1/3} k^{(\alpha+1)/3}. \quad (47)$$

This is a kinetic, phase-space analogue of the critical-balance conjecture in magnetohydrodynamic turbulence [70, 71].

Assuming a constant flux of δC_2 in position space, using the ℓ scaling in (46), and using (31) to relate fluctuations in real space and wavenumber space, we get

$$\begin{aligned} \frac{v_{\text{th}} \delta f_\ell^2}{\tau_c} \sim \varepsilon &\implies v_{\text{th}} \delta f_\ell^2 \sim \varepsilon \kappa^{-1/3} \ell^{(2-\alpha)/3} \\ \iff L \int ds \hat{F} &\sim \varepsilon \kappa^{-1/3} k^{-(5-\alpha)/3}, \end{aligned} \quad (48)$$

where δf_ℓ is the characteristic amplitude of δf at spatial scale ℓ . Let us compare this result to the 1-D k spectrum that follows from (43). We assume (and verify *a posteriori*) that $b > 1$, so that the integral of \hat{F} over s is dominated by the region $\xi \gtrsim 1$, i.e.,

$$s \lesssim \kappa^{-1/3} k^{(\alpha+1)/3}. \quad (49)$$

This gives

$$\int ds \hat{F} \propto \int_0^{\kappa^{-1/3} k^{(\alpha+1)/3}} ds k^{-c} \propto k^{-c+(\alpha+1)/3}. \quad (50)$$

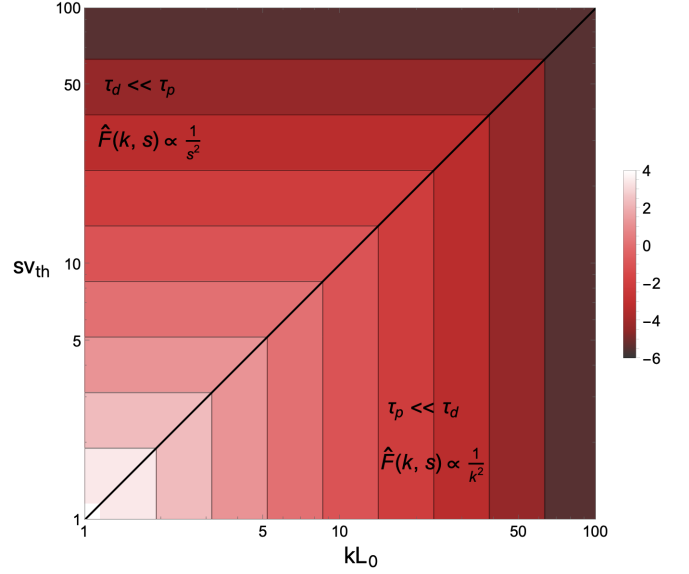


FIG. 1. Cartoon contour plot of $\log L_0^2 v_{\text{th}}^{6/(\alpha+1)} \hat{F}(kL_0, sv_{\text{th}})$ vs. (kL_0, sv_{th}) , for $\alpha = 2$, using the piecewise scalings (54). We use normalized units sv_{th} and kL_0 , where L_0 is defined in (91) (see the discussion at the beginning of Section VB). The black line is the critical-balance line (47), $sv_{\text{th}} \sim kL_0$. In the $\tau_p \ll \tau_d$ ($\xi \gg 1$) region, the spectrum scales as k^{-2} , and in the $\tau_d \ll \tau_p$ ($\xi \ll 1$) region, the spectrum scales as s^{-2} .

Requiring consistency between (50) and (48) yields $c = 2$.

We can now perform the same exercise in velocity space, viz.,

$$\begin{aligned} \frac{v_{\text{th}} \delta f_u^2}{\tau_c} \sim \varepsilon &\implies v_{\text{th}} \delta f_u^2 \sim \varepsilon \kappa^{-1/(\alpha+1)} u^{(2-\alpha)/(\alpha+1)} \\ \iff L \int dk \hat{F} &\sim \varepsilon \kappa^{-1/(\alpha+1)} s^{-3/(\alpha+1)}, \end{aligned} \quad (51)$$

where δf_u is the characteristic amplitude of δf at velocity scale u . On the other hand, using (43) and assuming that the integral over k of \hat{F} is dominated by the region $\xi \lesssim 1$, or

$$k \lesssim \kappa^{1/(\alpha+1)} s^{3/(\alpha+1)}, \quad (52)$$

we have

$$\int dk \hat{F} \propto \int_0^{\kappa^{1/(\alpha+1)} s^{3/(\alpha+1)}} dk s^{-b} \propto s^{-b+3/(\alpha+1)}. \quad (53)$$

Requiring consistency between (53) and (51) yields $b = 6/(\alpha + 1)$.

Assembling the scalings that we have surmised above, we find that the spectrum (43) is

$$\hat{F}(k, s) \sim \varepsilon L^{-1} \begin{cases} \kappa^{-2/(\alpha+1)} s^{-6/(\alpha+1)}, & \xi \ll 1, \\ k^{-2}, & \xi \gg 1. \end{cases} \quad (54)$$

For $\alpha = 2$, this was derived, by means of a formal solution, in [35], but the phenomenological argument and

physical interpretation presented here are new. Note that the dimensional factors in (54) come from using Parseval's theorem (31) together with demanding that the integrals of the spectrum in (50) and (53) satisfy the constant-flux relations in position and velocity space, respectively, viz., (48) and (51). As an example, we plot the spectrum (54) for $\alpha = 2$ in Fig. 1.

In summary, we have constructed a phenomenological theory according to which δC_2 undergoes a phase-space cascade in both position and velocity space. At large k ($\xi \gg 1$), the spectrum is phase-mixing-dominated and has a power-law scaling in k . At large s ($\xi \ll 1$), the spectrum is turbulent-diffusion-dominated and has a power-law scaling in s . These two regimes are separated in phase space by the critical-balance region $\xi \sim 1$, where the linear and nonlinear time scales are comparable. The 1-D k and s spectra are dominated by contributions from this critical-balance region.

Since the collision operator is diffusive in velocity space and ν is assumed to be small, collisional dissipation must necessarily occur at fine velocity-space scales (large s). It is therefore unsurprising that a kinetic system with injection of a quadratic invariant exhibits a constant-flux cascade of that invariant in velocity space. However, there is no *a priori* scale in position space where the dissipation must happen, so it is nontrivial that there also exists a cascade in position space. This inertial range in position space emerges due to the nonlinear field-particle interactions in (33), which mix position and velocity space [35].

A reader interested in how the above results are obtained more rigorously should read Sections IV and V, where we solve (33) properly for the spectrum and fluxes of δC_2 . A reader interested only in the big picture can skip straight to Section VI.

IV. PHASE-SPACE FLUXES

We now verify the phenomenological theory presented in Section III by solving (33). It is useful to write this equation in flux-gradient form:

$$\frac{\partial \hat{F}}{\partial t} + \nabla \cdot \hat{\Gamma} = \hat{S} - 2\nu s^2 \hat{F}, \quad (55)$$

where $\nabla = (\partial/\partial k, \partial/\partial s)$ is a gradient operator in the (k, s) space, and the flux $\hat{\Gamma} = (\hat{\Gamma}^k, \hat{\Gamma}^s)$ has components

$$\hat{\Gamma}^s = k \hat{F}, \quad (56)$$

which is clear from (33), and

$$\hat{\Gamma}^k = i \kappa s^2 \frac{1}{L} \int_{-\infty}^{+\infty} dr e^{-ikr} \frac{|r|^\alpha}{r} F(r, s). \quad (57)$$

The latter expression can be derived using (36), viz., by writing the Fourier transform of the nonlinear term as

$$\kappa s^2 |r|^\alpha F(r, s) = -ir \left[i \kappa s^2 \frac{|r|^\alpha}{r} F(r, s) \right]. \quad (58)$$

Inverse-Fourier transforming the term in brackets in (58) yields (57) [53]. In steady state, (55) reads

$$\nabla \cdot \hat{\Gamma} = k \frac{\partial \hat{F}}{\partial s} + \kappa s^2 (-\Delta_k)^{\alpha/2} \hat{F} = \hat{S} - 2\nu s^2 \hat{F}. \quad (59)$$

In Sections IV A and IV B, we compute $\hat{\Gamma}^k$ and $\hat{\Gamma}^s$ integrated over s and k , respectively. Then, in Section V, we compute the spectrum $\hat{F}(k, s)$ and analyze the full flux $\hat{\Gamma}$ in (k, s) space. This order of presentation may seem awkward, but is, in fact, necessary. This is because the integrated fluxes inform us of the nature of the solution of (59). This solution is in turn needed to compute the 2-D flux in (k, s) space.

A. Constant flux in k

Let us integrate (59) over all s . The s flux vanishes at $s \rightarrow \pm\infty$, and we are left with an equation for $\hat{g}(k) = \int_{-\infty}^{+\infty} ds s^2 \hat{F}$, which satisfies

$$\kappa (-\Delta_k)^{\alpha/2} \hat{g} = \hat{S} - 2\nu \hat{g}, \quad (60)$$

where $\hat{S}(k) = \int_{-\infty}^{+\infty} ds \hat{S}(k, s)$. This integrated source \hat{S} injects \hat{g} , which is diffused by the nonlinear term and dissipated by collisions.

The source (34) is peaked at low k , with characteristic width L_E^{-1} . To analyze the behavior of $\hat{g}(k)$ in the region $kL_E \gg 1$, we approximate $\hat{S}(k) \approx (\varepsilon/L) \delta(k)$. Fourier transforming (60) and solving for $g(r)$, the Fourier transform of $\hat{g}(k)$, yields

$$g(r) = \frac{\varepsilon}{2\pi\kappa} \frac{1}{|r|^\alpha + \ell_\nu^\alpha}, \quad (61)$$

whence

$$\hat{g}(k) = \frac{1}{L} \int dr e^{-ikr} g(r) = \frac{\varepsilon}{2\pi\kappa L} \int dr \frac{e^{-ikr}}{|r|^\alpha + \ell_\nu^\alpha}, \quad (62)$$

where we have defined the 'Kolmogorov' (dissipation) scale as

$$\ell_\nu \equiv \left(\frac{2\nu}{\kappa} \right)^{1/\alpha}. \quad (63)$$

For $\alpha = 2$, (62) simplifies to

$$\hat{g}(k) = \frac{\varepsilon}{2\pi\kappa L} \int dr \frac{e^{-ikr}}{r^2 + \ell_\nu^2} = \frac{\varepsilon \ell_\nu}{4\nu L} e^{-|k|\ell_\nu}. \quad (64)$$

For $\alpha < 2$, (62) does not have a simple closed-form expression, but it can be manipulated into an integral where the exponential in the integrand is decaying rather than oscillatory:

$$\hat{g}(k) = \frac{\varepsilon \ell_\nu}{2\pi\nu L} \int_0^\infty dz \frac{\sin(\pi\alpha/2) z^\alpha}{z^{2\alpha} + 2z^\alpha \cos(\pi\alpha/2) + 1} e^{-|k|\ell_\nu z}. \quad (65)$$

This will be useful in what follows. Deriving (65) from (62) requires some work, which is done in Appendix C.

The solution (62) implies that the rate of δC_2 injection by the source equals the rate of δC_2 dissipation by collisions. Indeed, using (32) and (62), and converting the sums over k into integrals, the collisional dissipation can be written in terms of \hat{g} :

$$2\nu L \int dk \hat{g}(k) = 2\nu \int dk \frac{\varepsilon}{2\pi\kappa} \int dr \frac{e^{-ikr}}{|r|^\alpha + \ell_\nu^\alpha} \\ = \varepsilon \ell_\nu^\alpha \int dr \delta(r) \frac{1}{|r|^\alpha + \ell_\nu^\alpha} = \varepsilon = L \iint dk ds \hat{S}, \quad (66)$$

as expected. Since (62) is a Green's function solution to (60), it is straightforward to show that this balance also holds for arbitrary $\hat{S}(k)$. Importantly, (66) applies even in the limit $\nu \rightarrow 0^+$; emergence of such finite collisional dissipation in the collisionless limit is known as a dissipative anomaly [29]. This result, although perhaps obvious from the steady state of (32), demonstrates constructively that the steady-state solution to (55) is well defined in the collisionless limit.

Using the solution (61), we can now compute the 1-D k flux of δC_2 , viz., from (57),

$$L \int ds \hat{\Gamma}^k = i\kappa \int_{-\infty}^{+\infty} dr e^{-ikr} \frac{|r|^\alpha}{r} g(r). \quad (67)$$

For $\alpha = 2$, this flux reduces to

$$L \int ds \hat{\Gamma}^k = -L\kappa \frac{\partial \hat{g}}{\partial k} = \text{sgn}(k) \frac{\varepsilon}{2} e^{-|k|\ell_\nu}, \quad (68)$$

where we used the solution (64). For $\alpha < 2$,

$$L \int ds \hat{\Gamma}^k \\ = \text{sgn}(k) \frac{\varepsilon}{\pi} \int_0^\infty dz \frac{\sin(\pi\alpha/2) z^{\alpha-1}}{z^{2\alpha} + 2z^\alpha \cos(\pi\alpha/2) + 1} e^{-|k|\ell_\nu z}. \quad (69)$$

The derivation of (69) can be found in Appendix C. When $k\ell_\nu \ll 1$, both (68) and (69) are constant and equal to $\text{sgn}(k) \varepsilon/2$ (in this limit, the integral over z in (69) is $\pi/2$, which is also shown in Appendix C). This result, one of the most important of this paper, means there is a constant-flux cascade in position space, viz., there exists an inertial range, $1/L_E \ll k \ll 1/\ell_\nu$, unaffected directly by forcing or collisions, where δC_2 is transferred from larger to smaller scales.

At $k\ell_\nu \gtrsim 1$, collisions become relevant. The dissipation rate at scales $\gtrsim 1/k$ is

$$\hat{D}(k) = 2\nu L \int_{-k}^{+k} dk' \hat{g}(k'). \quad (70)$$

Substituting (64) or (65) into (70) gives, for $\alpha = 2$,

$$\hat{D}(k) = \frac{\varepsilon \ell_\nu}{2} \int_{-k}^{+k} dk' e^{-|k'|\ell_\nu} = \varepsilon (1 - e^{-k\ell_\nu}) \quad (71)$$

or, for $\alpha < 2$,

$$\hat{D}(k) = \frac{2\varepsilon}{\pi} \int_0^\infty dz \frac{\sin(\pi\alpha/2) z^{\alpha-1}}{z^{2\alpha} + 2z^\alpha \cos(\pi\alpha/2) + 1} (1 - e^{-k\ell_\nu z}). \quad (72)$$

From (71) and (72), we see that the collisional dissipation is only order-unity when $k\ell_\nu \gtrsim 1$, i.e., below the Kolmogorov scale (63), which, therefore, deserves the name that we have given it. Past $k\ell_\nu \gtrsim 1$, the dissipation balances the δC_2 injected by the forcing ($\hat{D}(k) \simeq \varepsilon$ when $k\ell_\nu \gg 1$; derived in Appendix C). As discussed at the end of Section III, because the collision operator is diffusive in velocity space, there is no *a priori* scale in position space where the dissipation must happen. Rather, this dissipation range in position space forms because of the collisionless dynamics. Note that $\ell_\nu \rightarrow 0$ as $\nu \rightarrow 0$, so arbitrarily fine-scale structure in position space can be generated in the collisionless limit. Because of the constant-flux cascade, all of the δC_2 injected at large scales reaches the dissipation range, no matter how small ℓ_ν is.

B. Constant flux in s

Let us now integrate (59) over all k . The k flux vanishes at $k \rightarrow \pm\infty$, resulting in the following equation for the s flux:

$$\frac{\partial}{\partial s} \int dk \hat{\Gamma}^s = \int dk \hat{S} - 2\nu s^2 \int dk \hat{F}. \quad (73)$$

Unfortunately, unlike (60), this equation is not closed and cannot be explicitly solved without knowing the spectrum itself. However, we can still learn a key lesson from it. In view of (34) and (35), the characteristic width over which $\int dk \hat{S}$ falls off in s is $1/v_{\text{th}}$. But for small ν , collisions can only be relevant when s is large. Balancing the phase-mixing term with the collision term in (59) tells us that collisions will start to matter when

$$\frac{k}{s} \sim \nu s^2. \quad (74)$$

We know from Section IV A that collisional dissipation will start to occur around $k\ell_\nu \sim 1$, so taking $k \sim 1/\ell_\nu$ in (74) gives us the collisional velocity scale

$$u_\nu \sim \left(\frac{\nu^{\alpha+1}}{\kappa} \right)^{1/3\alpha}. \quad (75)$$

When $su_\nu \ll 1$, we expect that we can drop the collision term in (73). Integrating the remaining terms in the equation from $-s$ to s , where $1/v_{\text{th}} \ll s \ll 1/u_\nu$, yields, using (38),

$$\int dk \hat{\Gamma}^s(s) - \int dk \hat{\Gamma}^s(-s) \\ = \int_{-s}^{+s} ds' \int_{-\infty}^{+\infty} dk \hat{S}(k, s') \approx \text{sgn}(s) \frac{\varepsilon}{L}. \quad (76)$$

Because the distribution function is real, the Fourier spectrum satisfies

$$\hat{F}(k, -s) = \hat{F}^*(-k, s). \quad (77)$$

Together with the definition (56) of $\hat{\Gamma}^s$, this implies that $\int dk \hat{\Gamma}^s(-s) = -\int dk \hat{\Gamma}^s(s)$, and so (76) becomes

$$L \int dk \hat{\Gamma}^s(s) = \text{sgn}(s) \frac{\varepsilon}{2} \quad (78)$$

for $1/v_{\text{th}} \ll s \ll 1/u_\nu$. There is, therefore, also an inertial range in s where there is a constant flux of δC_2 from small to large $|s|$. Because the collision operator can only be relevant at large $|s|$ when ν is small, the existence of a forced steady state does indeed require such a constant-flux inertial range in s .

We note that this result holds even in the absence of nonlinearity. Linear phase mixing can lead to the development of arbitrarily fine scales in velocity space, albeit at the price of a diverging δC_2 as $\nu \rightarrow 0^+$ [51]. However, nonlinearity is required for there to be a cascade in position space: note from (63) that $\ell_\nu \rightarrow \infty$ as $\kappa \rightarrow 0$. Indeed, the solution of (60) for $\kappa = 0$ is simply $\hat{g} = \hat{S}(k)/2\nu$. The Vlasov equation is linear in this limit, so the spatial Fourier components of the distribution function are uncoupled from one another, and the k dependence of the Fourier spectrum is then simply set by the source.

V. PHASE-SPACE SPECTRUM

We now compute the spectrum in (59). From Sections IV A and IV B, we know that our model exhibits a phase-space entropy cascade in which the rate of δC_2 injection by the forcing at large scales is balanced by collisional dissipation at small scales, with the distribution function developing arbitrarily small scales in phase space in the limit $\nu \rightarrow 0^+$. This results in an inertial range in k (s) where the flux of δC_2 integrated over velocity (position) wavenumbers is constant. Therefore, in this inertial range, viz., for $1/L_E \ll k \ll 1/\ell_\nu$ and $1/v_{\text{th}} \ll s \ll 1/u_\nu$, we can meaningfully consider (59) in the absence of the forcing and collisional terms, viz.,

$$k \frac{\partial \hat{F}}{\partial s} = -\kappa s^2 (-\Delta_k)^{\alpha/2} \hat{F}, \quad (79)$$

and seek a solution for the spectrum that supports constant fluxes in k and s .

A. Self-similar inertial-range solution

Because of the reality condition (77), we only need to solve (79) for $\hat{F}(k, s)$ on half of the (k, s) plane. We choose to solve for the spectrum in the upper half-plane, $-\infty < k < \infty$ and $s \geq 0$ [72].

To deal with the fractional Laplacian, we Fourier transform this equation in k space. Using (36), we find that $F(r, s)$ satisfies

$$\frac{\partial}{\partial r} \frac{\partial}{\partial s} F = -i\kappa s^2 |r|^\alpha F. \quad (80)$$

Because $F(r, s)$ is the Fourier transform of $\hat{F}(k, s)$, which is purely real, $F(r, s)$ must satisfy the reality conditions $F(-r, s) = F^*(r, s)$. We therefore only have to solve (80) for $r > 0$, for which $|r| = r$.

The inertial-range solution to (80) that does not depend on details of the forcing or dissipation ranges is a similarity solution [73]:

$$F = \varepsilon \kappa^{-1/(\alpha+1)} s^{-\beta} \phi(y), \quad y = (\kappa s^3)^{1/(\alpha+1)} r, \quad (81)$$

where β can be constrained by the fact that the flux $L \int dk \hat{\Gamma}^s$ must be constant in the inertial range, as per (78):

$$\begin{aligned} L \int dk \hat{\Gamma}^s &= \varepsilon s^{-\beta+3/(\alpha+1)} \int_{-\infty}^{+\infty} d\xi \xi \int_{-\infty}^{+\infty} dy e^{-i\xi y} \phi(y) = \frac{\varepsilon}{2}, \\ \implies \beta &= \frac{3}{\alpha+1}. \end{aligned} \quad (82)$$

The integration variable dual to y ,

$$\xi = \frac{k}{(\kappa s^3)^{1/(\alpha+1)}}, \quad (83)$$

has previously appeared in (42) as the ratio of the turbulent-diffusion and phase-mixing time scales.

Substituting (81) into (80) gives us an ordinary differential equation for ϕ :

$$\frac{d^2 \phi}{dy^2} + i \frac{(\alpha+1)}{3} y^{\alpha-1} \phi = 0. \quad (84)$$

To solve this equation, consider the transformation

$$\phi = \sqrt{y} g(z), \quad z = \frac{2}{\sqrt{3(\alpha+1)}} e^{-i\pi/4} y^{(\alpha+1)/2}. \quad (85)$$

Then, (84) becomes a modified Bessel equation [74]:

$$z^2 \frac{d^2 g}{dz^2} + z \frac{dg}{dz} - \left[z^2 + \frac{1}{(\alpha+1)^2} \right] g = 0. \quad (86)$$

Therefore, the solution to (84) that vanishes at $y \rightarrow \infty$ is

$$\phi(y) = \Lambda \sqrt{y} K_{1/(\alpha+1)} \left(\frac{2}{\sqrt{3(\alpha+1)}} e^{-i\pi/4} y^{(\alpha+1)/2} \right), \quad (87)$$

where $y > 0$, K is the modified Bessel function of the second kind, and Λ is a constant. The reality condition $\phi(y) = \phi^*(-y)$ constrains us to pick the phase of Λ so

that the real part of ϕ is even in y and the imaginary part is odd. This is accomplished by setting

$$\Lambda = \sigma(e^{-i\pi/4})^{1/(\alpha+1)}, \quad (88)$$

where $\sigma > 0$ is real and determined by the constraint (82). For generic α , we are unable to evaluate the integrals in (82) analytically, to compute σ , although it is straightforward to see that σ is finite. For $\alpha = 1$, σ is easily computed: this calculation can be found in Appendix D.

Using the solution (87) for ϕ , we inverse-Fourier transform back to k space to obtain,

$$\hat{F}(k, s) = 2\varepsilon L^{-1} \kappa^{-2/(\alpha+1)} s^{-6/(\alpha+1)} \operatorname{Re} \int_0^\infty dy e^{-i\xi y} \phi(y), \quad (89)$$

where ξ is given by (83), and we have used the reality condition for ϕ . As we stated at the beginning of this calculation, this expression is valid only for $s \geq 0$; the spectrum for negative s can be found by combining (77) and (89). For generic α , we are unable to simplify (89) further. For $\alpha = 1$, (89) has a simple closed form, derived in Appendix D. For $\alpha = 2$, the spectrum can be written in terms of incomplete Gamma functions: see [35]. In our terms, (87) for $\alpha = 2$ reduces to

$$\phi(y) = \sigma\pi\sqrt{3}\operatorname{Ai}\left(e^{-i\pi/6}y\right), \quad (90)$$

where Ai is the Airy function. This is clear by the fact that for $\alpha = 2$, (84) is an Airy equation.

B. 2-D spectrum

To show what (89) looks like, we present contour plots of the normalized spectrum $L_0^2 v_{\text{th}}^{6/(\alpha+1)} \hat{F}(kL_0, sv_{\text{th}})$ for $\alpha = 1$ (for which an explicit expression can be found in Appendix D) in Fig. 2. We use normalized units sv_{th} and kL_0 , where

$$L_0 = \left(\frac{v_{\text{th}}^3}{\kappa}\right)^{1/(\alpha+1)}. \quad (91)$$

This length scale is a natural choice, because the similarity variable (83) in these units is

$$\xi = \frac{k}{(\kappa s^3)^{1/(\alpha+1)}} = \frac{kL_0}{(sv_{\text{th}})^{3/(\alpha+1)}}, \quad (92)$$

and, therefore, the spectrum, up to its amplitude, is independent of κ .

For $\xi \sim 1$, the spectrum is a nontrivial function of k and s . For ξ small or large, it has asymptotics given by (54) (computed below), confirming the phenomenological theory presented in Section III. As discussed in Section III, the distinction between ξ small and large

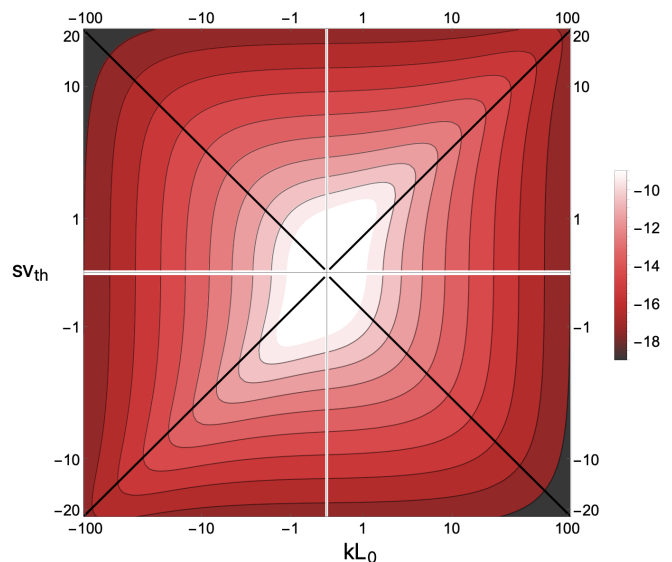


FIG. 2. Contour plot of $\log L_0^2 v_{\text{th}}^{6/(\alpha+1)} \hat{F}(kL_0, sv_{\text{th}})$ vs. (kL_0, sv_{th}) , for $\alpha = 1$. Note that the spectrum for $s < 0$ is given by the reality condition (77), $\hat{F}(k, s) = \hat{F}(-k, -s)$. The black lines are the critical-balance lines (47), $sv_{\text{th}} = \pm |kL_0|^{2/3}$. In order to use logarithmic axes, we do not plot the spectrum along the $k = 0$ and $s = 0$ axes. We have also not plotted the spectrum near the (k, s) origin, as the similarity solution (89) diverges there.

can be understood in terms of competition between the phase mixing and turbulent diffusion for control of the phase-space cascade.

To compute the asymptotics (54) from the full solution (89), the $\xi \ll 1$ limit can be found by simply setting $\xi = 0$ in (89). For the $\xi \gg 1$ limit, we use the following result from Fourier analysis. Suppose $u(y)$ is a function that is smooth for $y > 0$ and has the scaling $u(y) \sim y^{\lambda-1}$ as $y \rightarrow 0^+$, where $\lambda > 0$. Then

$$\int_0^\infty dy e^{-i\xi y} u(y) = \frac{\Gamma(\lambda)}{(i\xi)^\lambda} + o(\xi^{-\lambda}) \quad (93)$$

as $\xi \rightarrow \infty$ [75]. Note that (87) has the series

$$\phi(y) = A - B(e^{-i\pi/2})^{1/(\alpha+1)}y + \mathcal{O}(y^{\alpha+1}) \quad (94)$$

as $y \rightarrow 0^+$, where A and B are real and positive constants. Combining (93) and (94), one finds that the contribution to the integral in (89) from the constant part of (94) is purely imaginary and so vanishes. The next-order term from the linear part of (94) has a real component; the integral is therefore $\mathcal{O}(\xi^{-2})$ (since $\lambda = 2$), hence $\hat{F}(k, s) \propto k^{-2}$ as $\xi \rightarrow \infty$.

Note that, the 1-D k and s spectra, which can be found by integrating out the similarity variable ξ in (89), agree with (48) and (51).

Before continuing, it is instructive to assess the region of validity of (89) in the (k, s) plane. This spectrum is infrared-divergent and thus breaks down as

$(k, s) \rightarrow (0, 0)$; information about the functional form of the source (34), which would regularize the spectrum at long wavelengths, is lost by construction in the similarity solution (however, (89) does contain information about the flux from the source via the constraint (82)). Of course, the inertial-range spectrum is no longer valid in the region where the source (34) is concentrated, viz., when $sv_{\text{th}} \lesssim 1$ and $kL_E \lesssim 1$. For these reasons, we have not plotted the spectrum near the origin in the (k, s) plane in Fig. 2, and likewise for the fluxes plotted in the following sections [76].

In addition to the solution (89) lacking an outer scale, the approximation that the nonlinear term is a fractional Laplacian to lowest order also breaks down when $kL_E \lesssim 1$. This is clear in the derivation of the nonlinear term in Appendix B 4, where the fractional Laplacian emerges as the lowest-order term when $kL_E \gg 1$. Yet, away from $s = 0$, (89) is, in fact, continuous across $k = 0$. By dropping the finite- kL_E corrections in (33), we have shrunk the boundary layer $kL_E \lesssim 1$ to the point $k = 0$ [77].

We can also now address the concern of the lack of locality in k space of the source term (34) and whether dropping this term in the inertial range was justified, as discussed at the end of Section II C. Consider the two asymptotic regions, $\xi \ll 1$ and $\xi \gg 1$ (assuming also $sv_{\text{th}} \gg 1$, $su_\nu \ll 1$, and $k\ell_\nu \ll 1$). In the former region, the nonlinear term is dominant over the phase-mixing term, as per (44). Balancing the nonlinear term with (34) yields an inhomogeneous contribution to $\hat{F} \propto \langle \hat{f} \rangle^2$. Since $sv_{\text{th}} \gg 1$, this term is strongly suppressed, e.g., exponentially so in the case of a Maxwellian initial condition [see (35)], so this term is negligible compared to the $\xi \ll 1$ asymptotic in (54). In the latter region ($\xi \gg 1$), the phase-mixing term is dominant over the nonlinear term, as per (45). Balancing the phase-mixing term with (34) yields an inhomogeneous contribution to $\hat{F} \propto \hat{D}(k)/k$, which is $\propto k^{-(2+\alpha)}$ when $kL_E \gg 1$. This contribution is subdominant to the homogeneous part of the spectrum, which scales like k^{-2} when $\xi \gg 1$, viz., (54). We cannot explicitly estimate the inhomogeneous contribution to the spectrum from the source in the $\xi \sim 1$ region, but the above analysis suggests it should be subdominant to (89). Therefore, even though the source is multiscale in k , there is still an inertial range in the position space.

Finally, we observe that the inertial-range solution (89) extends to infinity, consistent with $k_\nu \sim 1/\ell_\nu \rightarrow \infty$ and $s_\nu \sim 1/u_\nu \rightarrow \infty$ as $\nu \rightarrow 0^+$, viz., (63) and (75). A finite ν will introduce finite collisional scales k_ν and s_ν , such that collisions cut off the spectrum when $k \gtrsim k_\nu$ and $s \gtrsim s_\nu$.

C. 2-D flux: phase-space circulations

To gain insight about the pathways in phase space taken by \hat{F} from injection to dissipation scales, it is informative to examine the vector flux $\hat{\Gamma}$, which, in terms

of the similarity solution (89), has the components (57),

$$\hat{\Gamma}^k(k, s) = -2\varepsilon L^{-1} s^{-1} \text{Im} \int_0^\infty dy e^{-i\xi y} y^{\alpha-1} \phi(y), \quad (95)$$

and (56),

$$\begin{aligned} \hat{\Gamma}^s(k, s) \\ = 2\varepsilon L^{-1} \kappa^{-1/(\alpha+1)} s^{-3/(\alpha+1)} \xi \text{Re} \int_0^\infty dy e^{-i\xi y} \phi(y). \end{aligned} \quad (96)$$

To obtain (95), we used (81) and changed variables from r to y in the integral. Note that these expressions are valid only for $s \geq 0$. For $s < 0$, combining (56), (57), and (77), we have that

$$\hat{\Gamma}(k, -s) = -\hat{\Gamma}(-k, s). \quad (97)$$

As was the case for the Fourier spectrum, the flux is a nontrivial function of k and s for $\xi \sim 1$, but can be simplified when ξ is small or large. The asymptotics of the k and s components of the flux, which we derive below, are

$$\begin{aligned} \hat{\Gamma}^k(k, s) &\sim \varepsilon L^{-1} \\ &\times \begin{cases} -s^{-1}, & \xi \ll 1, \\ \text{sgn}(k) \kappa^{\alpha/(\alpha+1)} |k|^{-\alpha} s^{(2\alpha-1)/(\alpha+1)}, & \xi \gg 1, \quad \alpha < 2, \\ \kappa k^{-3} s^2, & \xi \gg 1, \quad \alpha = 2. \end{cases} \end{aligned} \quad (98)$$

and

$$\hat{\Gamma}^s(k, s) \sim \varepsilon L^{-1} \begin{cases} \kappa^{-2/(\alpha+1)} k s^{-6/(\alpha+1)}, & \xi \ll 1, \\ k^{-1}, & \xi \gg 1, \end{cases} \quad (99)$$

respectively. Here, we have retained the signs of terms as well as dimensional factors in (98) and (99), but not order-unity constants. To evaluate the asymptotics of the fluxes for $s < 0$, these expressions must be combined with (97).

We can derive these results in the same way as we did the asymptotics of the spectrum in Section V B. The asymptotics (99) for $\hat{\Gamma}^s$ come directly from combining (56) and (54). For $\hat{\Gamma}^k$, the $\xi \ll 1$ expansion in (98) comes from evaluating (95) at $\xi = 0$ (note that the integral is positive). For $\xi \gg 1$, we can combine (93), (94), and (95). This gives, to lowest order, as $\xi \rightarrow \infty$,

$$\hat{\Gamma}^k \simeq 2\varepsilon L^{-1} s^{-1} A \Gamma(\alpha) \sin\left(\frac{\pi\alpha}{2}\right) \text{sgn}(k) |\xi|^{-\alpha}. \quad (100)$$

The lowest-order k flux vanishes when $\alpha = 2$, so (100) only gives the $\xi \gg 1$ limit in (98) for $\alpha < 2$. We need to go to next order for $\alpha = 2$, which yields

$$\hat{\Gamma}^k \simeq 2\varepsilon L^{-1} s^{-1} B \Gamma(3) \sin\left(\frac{\pi}{3}\right) \text{sgn}(k) |\xi|^{-3}, \quad (101)$$

giving the $\xi \gg 1$, $\alpha = 2$ asymptotic in (98).

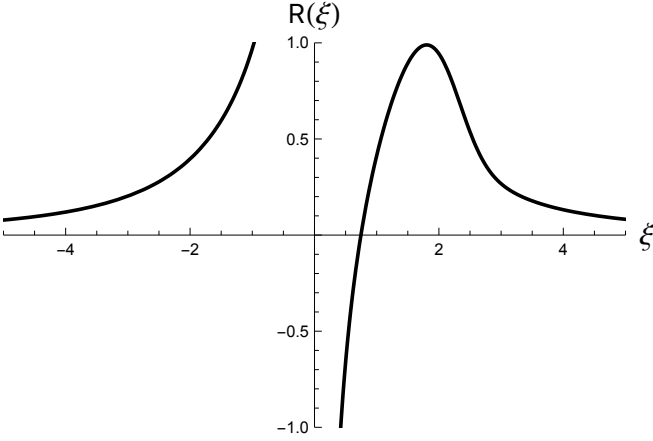


FIG. 3. The ratio (103) versus ξ for $\alpha = 2$, calculated by numerically integrating (89). The point where R vanishes, $\xi = \xi_2 \simeq 0.747$, corresponds to $\hat{\Gamma}^k = 0$.

We first discuss the Batchelor case ($\alpha = 2$), where

$$(\hat{\Gamma}^k, \hat{\Gamma}^s) = \left(-\kappa s^2 \frac{\partial \hat{F}}{\partial k}, k \hat{F} \right). \quad (102)$$

To work out by what physical mechanism the phase-space cascade is enabled in different parts of the (k, s) plane, it is useful to compare the ratio of the k and s fluxes. Using the normalizations from Section VB, we have that the ratio of the dimensionless fluxes is

$$R = \frac{L_0^4 \hat{\Gamma}^k(kL_0, sv_{\text{th}})}{L_0^2 v_{\text{th}}^2 \hat{\Gamma}^s(kL_0, sv_{\text{th}})} = -\frac{1}{\xi} \frac{\text{Im} \int_0^\infty dy e^{-i\xi y} y \phi(y)}{\text{Re} \int_0^\infty dy e^{-i\xi y} \phi(y)}, \quad (103)$$

which is a function solely of ξ . It has the asymptotics

$$R \sim \begin{cases} -\xi^{-1}, & \xi \ll 1, \\ \xi^{-2}, & \xi \gg 1. \end{cases} \quad (104)$$

Thus, when $\xi \ll 1$, the flux is diffusion-dominated (dominated by its k component), and when $\xi \gg 1$, the flux is phase-mixing-dominated (dominated by its s component). When $\xi \sim 1$, the two fluxes are comparable; this can be seen in the plot of R in Fig. 3. The regions of the dominance of the two fluxes are, therefore, separated in phase space by the critical-balance line (47), the same as the phase-mixing and turbulent-diffusion time scales, viz., (42).

We plot the (nondimensionalized) vector flux (102) in Fig. 4(a). Using the asymptotics (104) and noting the signs of the fluxes in (98) and (99), we see that in the diffusion-dominated region ($\xi \ll 1$), $\hat{\Gamma}^k$ is negative when $s > 0$ and positive when $s < 0$, and in the phase-mixing-dominated region ($\xi \gg 1$), $\hat{\Gamma}^s$ is positive when $k > 0$ and negative when $k < 0$. The flux therefore gives rise to counterclockwise circulation of δC_2 in (k, s) space. The sign changes in the components of the flux that enable this circulation occur at $\xi = \xi_2 \simeq 0.747$,

where R has a zero (as can be seen in Fig. 3), and at $\xi = 0$, below (above) which R diverges positively (negatively). The first point corresponds to $\hat{\Gamma}^k$ changing sign in the top right and bottom left quadrants, while the second point corresponds to $\hat{\Gamma}^s$ changing sign from positive to negative between the top right and top left quadrants, as well as between the bottom left and bottom right quadrants. This latter effect occurs because, when $\text{sgn}(ks) = -1$, perturbations are phase unmixed rather than phase mixed, being advected to low $|s|$ rather than high $|s|$ [35, 61]. The phase-unmixing modes are a stochastic instantiation of the plasma-echo effect [62, 63].

While the phase unmixing does undo the phase mixing, we will see in Section VE that the flux of the phase-mixing modes outweighs that of the phase-unmixing ones, thus enabling the constant-flux cascade. In Fig. 4(a), this manifests in the fact that the circulation swirls outward. Indeed, in the top right (bottom left) quadrant, below (above) the line $\xi = \xi_2$ where $\hat{\Gamma}^k = 0$, there is a flux of δC_2 to both high $|k|$ and high $|s|$ simultaneously, toward the dissipation wavenumbers $k_\nu \sim 1/\ell_\nu$ and $s_\nu \sim 1/u_\nu$.

D. Non-local transport

We now examine the $\alpha < 2$ cases. The important difference compared to the Batchelor regime is that the k flux is now non-local in k space. Note that $\hat{\Gamma}^k$ can be written as [53] [78]

$$\hat{\Gamma}^k = \kappa s^2 \frac{c_\alpha}{\alpha} \int_0^\infty dp \frac{\hat{F}(k-p, s) - \hat{F}(k+p, s)}{p^\alpha}, \quad (105)$$

where c_α is given by (B19). The derivation of this expression is given in Appendix B5. The interpretation of (105) is that ‘particles’ (parcels of δC_2) cross the point (k, s) from points $(k \pm p, s)$, with cumulative probability $\propto p^{-\alpha}$. The particles undergo Lévy flights in k space, so the flux at a point (k, s) receives contributions not just from nearby particles taking small jumps but also from far-away ones taking large jumps.

The net effect is an enhancement of $\hat{\Gamma}^k$ compared to $\hat{\Gamma}^s$. For these cases, the ratio R of the nondimensionalized fluxes is

$$\begin{aligned} R &= \frac{L_0^4 \hat{\Gamma}^k(kL_0, sv_{\text{th}})}{L_0^2 v_{\text{th}}^{6/(\alpha+1)} \hat{\Gamma}^s(kL_0, sv_{\text{th}})} \\ &= -(sv_{\text{th}})^{(2-\alpha)/(\alpha+1)} \frac{1}{\xi} \frac{\text{Im} \int_0^\infty dy e^{-i\xi y} y^{\alpha-1} \phi(y)}{\text{Re} \int_0^\infty dy e^{-i\xi y} \phi(y)}. \end{aligned} \quad (106)$$

Since $\hat{\Gamma}^k$ is positive when $\xi \gg 1$ and negative when $\xi \ll 1$, viz., (98), there is always an order-unity ξ_α at which $\hat{\Gamma}^k = 0$. Unlike the Batchelor case (103), the ratio of fluxes (106) is not a function solely of ξ . Therefore, (106) implies that along curves of constant $\xi \sim 1 \neq \xi_\alpha$, the flux

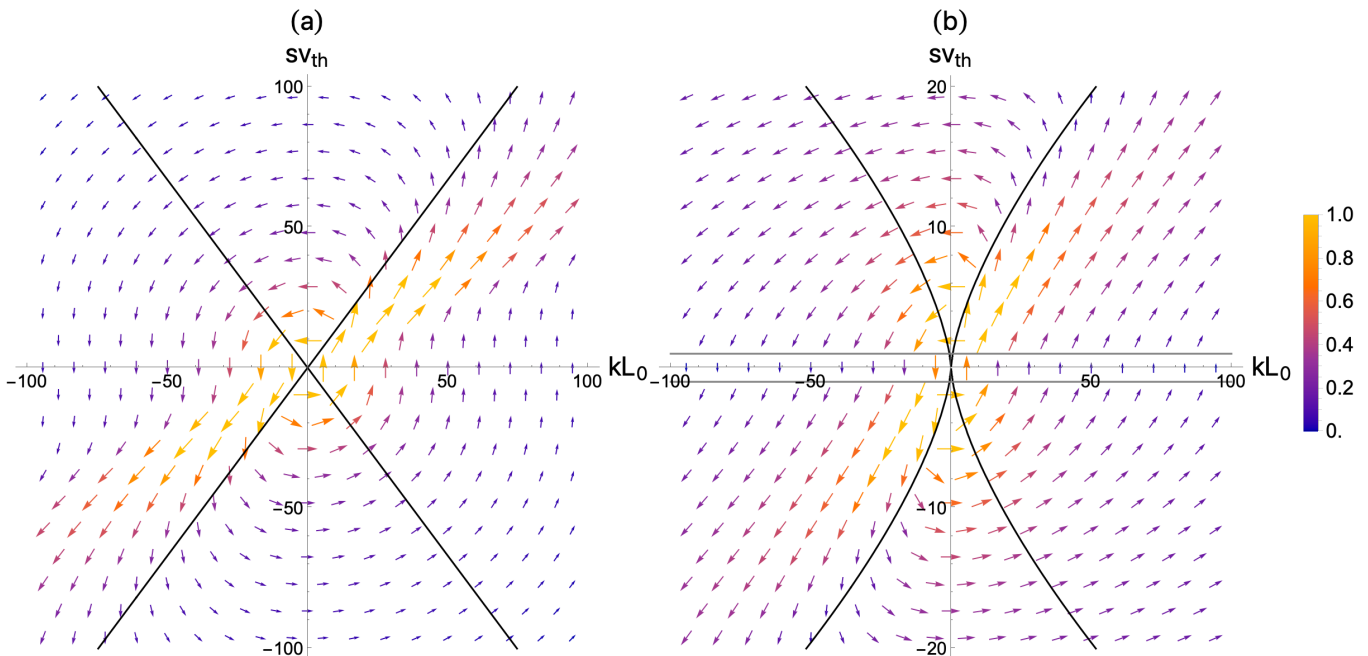


FIG. 4. (a) 2-D nondimensionalized flux for $\alpha = 2$, with k component $L_0^4 \hat{\Gamma}^k(kL_0, sv_{\text{th}})$ and s component $L_0^2 v_{\text{th}}^{6/(\alpha+1)} \hat{\Gamma}^s(kL_0, sv_{\text{th}})$, calculated by integrating (89) numerically. For emphasis, we specify the magnitude of the flux by both the length and color of the vectors. The black lines are the critical-balance lines (47) for these parameters, $sv_{\text{th}} = \pm kL_0/\xi_2$, where the slope $\xi_2 \simeq 0.747$ is chosen so that $\hat{\Gamma}^k$ vanishes along the line in the top right and bottom left quadrants. (b) The same as (a) but for $\alpha = 1$. Analytical expressions for the components of the flux in this case can be found in Appendix D, viz., (D6) and (D5). The black curves are the critical-balance lines (47) for these parameters, $sv_{\text{th}} = \pm |kL_0/\xi_1|^{2/3}$, where $\xi_1 = 1/\sqrt{3}$ is chosen so that $\hat{\Gamma}^k$ vanishes along the curve in the top right and bottom left quadrants [as can be seen in (D6)]. The gray lines are $sv_{\text{th}} = \pm 1$, bounding the only region, $|sv_{\text{th}}| \ll 1$, where the flux is phase-mixing-dominated (apart from the critical-balance curve).

is always diffusion-dominated as $sv_{\text{th}} \rightarrow \infty$. Furthermore, in the asymptotic region $\xi \gg 1$ (which for $\alpha = 2$ was the phase-mixing-dominated region), we show in Appendix E that, as α gets smaller, the region where the flux is asymptotically phase-mixing-dominated shrinks. In fact, for $\alpha < 1/2$, there is no asymptotic region at all where the flux is phase-mixing-dominated (except along the curve $\xi = \xi_\alpha$).

As an example, we plot the (nondimensionalized) vector flux for $\alpha = 1$ in Fig. 4(b) (explicit expressions for the components of the flux in this case can be found in Appendix D). In this case, apart from along the curve $\xi = \xi_1$ where $\hat{\Gamma}^k = 0$, the flux is phase-mixing-dominated only in the region $|sv_{\text{th}}| \lesssim 1$ (irrespective of k), which in Fig. 4(b) we indicate with gray lines.

These results do not mean that there is no effective phase mixing for these cases. The ratio (42) of nonlinear and linear time scales gives the relative local transport of δC_2 in s versus k space. While the non-local transport of δC_2 in k space dominates over its flux in s , locally, the phase-mixing time (40) of \hat{F} is still shorter than the diffusion time (41) when $\xi \gg 1$. This dominant local phase mixing is what sets up the lowest-order, constant-flux-in- s spectrum in the $\xi \gg 1$ region, viz., (45) and (54).

The fluxes also obey critical balance. It is straightforward

to show, using (98) and (99) with calculations analogous to (50) and (53), that the 1-D fluxes (69) and (78) are dominated by contributions from the critical-balance region (47) ($\xi \sim 1$). Even though the 2-D s flux is subdominant to the k flux, the fact that $L \int dk \hat{\Gamma}^s$ is constant in the s inertial range implies that phase mixing still provides an effective route to dissipation scales in velocity space.

E. Shell-averaged flux

To understand the net effect of having both phase-mixing modes that propagate from low to high $|s|$ and phase-unmixing modes that propagate from high to low $|s|$, it is useful to consider the flux shell-averaged in k ,

$$\bar{\Gamma} \equiv \left(\hat{\Gamma}^k(k, s) - \hat{\Gamma}^k(-k, s), \hat{\Gamma}^s(k, s) + \hat{\Gamma}^s(-k, s) \right). \quad (107)$$

Note that in 1D, shell averaging amounts simply to adding together contributions from $+k$ and $-k$. The flux (107) is defined so that the shell-averaged spectrum

$\bar{F} \equiv \hat{F}(k, s) + \hat{F}(-k, s)$ satisfies the equation

$$\frac{\partial \bar{F}}{\partial t} + \nabla \cdot \bar{\Gamma} = 2\hat{S} - 2\nu s^2 \bar{F}. \quad (108)$$

While the components of (107) depend on α , their (nondimensionalized) ratio does not (up to a prefactor). Note that, using (84) and integrating by parts, (95) can be rewritten as

$$\hat{\Gamma}^k(k, s) = 2\varepsilon L^{-1} s^{-1} \times \frac{3}{\alpha + 1} \text{Re} \left[\phi'(0^+) + \xi^2 \int_0^\infty dy e^{-i\xi y} \phi(y) \right], \quad (109)$$

where the derivative of ϕ is taken at $y \rightarrow 0^+$. Using (96) and (109), we get

$$\begin{aligned} \bar{R} &= \frac{L_0^4 \left[\hat{\Gamma}^k(kL_0, sv_{\text{th}}) - \hat{\Gamma}^k(-kL_0, sv_{\text{th}}) \right]}{L_0^2 v_{\text{th}}^{6/(\alpha+1)} \left[\hat{\Gamma}^s(kL_0, sv_{\text{th}}) + \hat{\Gamma}^s(-kL_0, sv_{\text{th}}) \right]} \\ &= \frac{3}{\alpha + 1} \frac{kL_0}{sv_{\text{th}}}. \end{aligned} \quad (110)$$

Remarkably, this expression is valid everywhere in the (k, s) plane, independent of ξ being small or large. The flux is radial at both large sv_{th} and large kL_0 . We plot $\bar{\Gamma}$ for $\alpha = 1$ in Fig. 5, which clearly exhibits this feature.

Note that the components of the shell-averaged flux are positive-definite. We are only able to show directly that this property holds for $\alpha = 1$; this calculation can be found in Appendix D. An argument as to why the fluxes are positive-definite for the general case is as follows. Since (110) is positive, the components of (107) are either both positive or both negative for all (k, s) in the inertial range (no sign reversals are possible, otherwise the flux would not be divergence-free in the inertial range: see (59)). If the components were negative-definite, there would be a sink at the origin. However, there is a source at the origin, so the shell-averaged fluxes must therefore be positive-definite.

This positive definiteness is important. The circulatory nature of the fluxes in Fig. 4 is due to phase-mixing modes (with $\text{sgn}(ks) = 1$) and phase-unmixing modes (with $\text{sgn}(ks) = -1$) propagating in opposite directions in s . Since the s component of (107) is equal to $k[\hat{F}(k, s) - \hat{F}(-k, s)]$, the shell-averaged flux being positive-definite means that the spectral amplitudes of the phase-mixing modes are greater than those of the phase-unmixing modes. Therefore, by adding together the fluxes of the two modes, we are left with a net flux that points outward to both high k and high s toward the dissipation scales, in agreement with our analysis in Sections VC and VD.

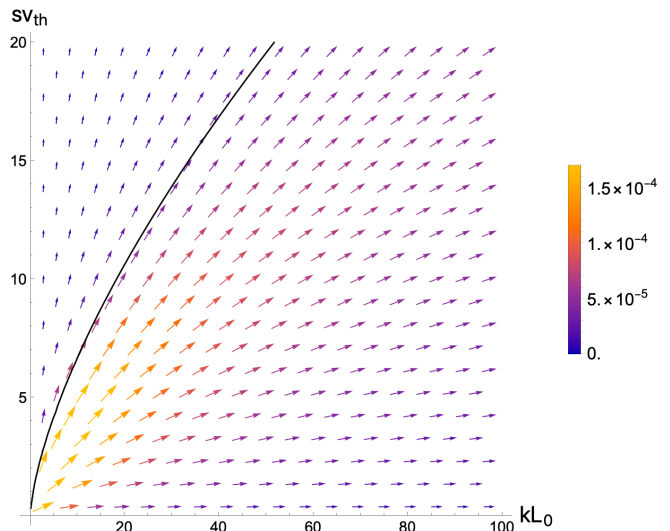


FIG. 5. 2-D nondimensionalized shell-averaged (in k) flux (107) for $\alpha = 1$, with k component $L_0^4 \bar{\Gamma}^k(kL_0, sv_{\text{th}})$ and s component $L_0^2 v_{\text{th}}^{6/(\alpha+1)} \bar{\Gamma}^s(kL_0, sv_{\text{th}})$. For emphasis, we specify the magnitude of the flux by both the length and color of the vectors. The black curve is the critical-balance curve (47) for these parameters, $sv_{\text{th}} = (kL_0/\xi_1)^{2/3}$, where $\xi_1 = 1/\sqrt{3}$.

VI. CONCLUSION

A. Summary

In this paper, we have presented a solvable model of kinetic plasma turbulence, in which the electric field is decoupled from the particle distribution function and taken to be an externally imposed Gaussian field, white-noise in time and power-law in k space.

The effect of this stochastic electric field on the mean distribution function is diffusion in velocity space, often referred to as stochastic heating [6, 40–42]. The resulting energization of particles is a collisionless process. Indeed, the heating rate is set by the turbulent collisionality and is independent of ν [see (15)]. However, the irreversibility of stochastic heating hinges on the presence of collisions. As $\langle f \rangle$ heats, δf fluctuations are excited, transferring the minus ‘entropy’ $C_{2,0} = (1/L) \int dx dv \langle f \rangle^2 / 2$ into $\delta C_2 = (1/L) \int dx dv \langle \delta f^2 \rangle / 2$, which then cascades to small scales in both position and velocity space simultaneously. This cascade is then cut off by collisions at fine phase-space scales, thereby rendering the heating irreversible. The irreversibility of stochastic heating is therefore enabled by the entropy cascade.

We have analyzed this cascade in the Fourier-transformed (k, s) space, where an ‘inertial range’ forms to bridge the injection and dissipation scales of δC_2 . Integrated over k or s , the flux of δC_2 is constant in this inertial range. Importantly, there is no collisional dissipation at scales much larger than the dissipation scale (ℓ_ν, u_ν) [see (63) and (75)], which tends to $(0, 0)$ as the

collision frequency does.

In the 2-D (k, s) space, the Fourier spectrum of δC_2 has a self-similar profile, with power-law asymptotics at high k and s , respectively. We find that these asymptotic scalings can be deduced by a phenomenological theory whose governing principle is that the cascade satisfies a critical balance in phase space between the time scales of linear phase mixing and turbulent diffusion. Because there is nothing in our phenomenological theory that is unique to 1D-1V, we also expect these ideas to apply in 2D-2V and 3D-3V. While the one-dimensional $|k|$ and $|s|$ spectra (48) and (51) should be the same, the two-dimensional $|k|$ - $|s|$ spectrum (integrated over angles) will not be the same as (54) because of the wavenumber Jacobian being different from unity in higher dimensions.

B. Fast cascade and the effectiveness of phase mixing

In a linear system, phase mixing acts as a route to collisional dissipation at every spatial scale [50, 51], but in the model presented here, collisional dissipation is only non-negligible below the dissipation scale ℓ_ν . Following the commonly held intuition that the effect of phase mixing (and Landau damping) on turbulent systems is that it steepens the spectrum (of, e.g., electromagnetic energy) at every scale by an amount set by the Landau-damping rate [27, 79–84], one may be led to conclude from our results that phase mixing is less effective in a nonlinear system than in a linear one. However, in fact, phase mixing is even more effective in a nonlinear system. This is because the presence of nonlinearity produces fine structure in position space and thus enhances the rate at which the distribution function develops fine phase-space gradients, reducing the time that it takes collisions to activate, τ_ν .

To see this, note that in a steadily driven system, as considered in this paper, the total δC_2 in steady state divided by the injection rate ε gives a reasonable estimate for τ_ν . For a linear system, restricting ourselves to a single k and noting that the spectrum is flat in s [85] up to a collisional cutoff $s_\nu \propto \nu^{-1/3}$ given by the balance (74) [50, 51], we find [86]

$$\tau_\nu \sim \frac{\delta C_2}{\varepsilon} \propto \int^{s_\nu} ds \propto \nu^{-1/3}. \quad (111)$$

For smaller and smaller ν , it takes longer and longer for collisions to dissipate the velocity-space structure of the distribution function, and in the collisionless limit, the amount of δC_2 stored in phase space diverges [51]. This is consistent with a constant cascade time, set by the phase-mixing time, viz., $\tau_c \sim (k v_{\text{th}})^{-1}$ (with k fixed).

In the presence of nonlinearity, when $\alpha = 2$, the 1-D spectra (48) and (51) scale like k^{-1} and s^{-1} , respectively [35], the former scaling in agreement with the classical Batchelor [65] spectrum of a passive scalar advected by a single-scale flow. Integrating the 1-D spectrum up

to the collisional cutoff (63) gives

$$\tau_\nu \sim \frac{\delta C_2}{\varepsilon} \propto \int^{1/\ell_\nu} dk k^{-1} \propto |\log \nu|. \quad (112)$$

Although formally also divergent as $\nu \rightarrow 0^+$, (112) is asymptotically shorter than (111). In this case, the cascade time is also constant, viz., $\tau_c \sim \kappa^{-1/3}$, as can be seen in (46), even though many k 's are involved.

When $\alpha < 2$, the phase-space cascade is even more efficient. From (46), we have that τ_c goes to zero as k and s go to infinity, so fluctuations ‘turn over’ faster to finer phase-space scales the deeper they are in the inertial range (compared to the constant cascade times in the linear and Batchelor regimes). As a result, the 1-D spectra (48) and (51) are steeper than k^{-1} and s^{-1} , so the total steady-state δC_2 and τ_ν are independent of ν .

Thus, the presence of nonlinearity reduces the collision time from a (negative) fractional power of ν (111) in the linear regime to a time scale that is only logarithmic with ν (112) when $\alpha = 2$, or one that is independent of ν when $\alpha < 2$. To interpret this shortening of τ_ν in the nonlinear regime, note that linear phase mixing still processes δC_2 from injection to dissipation scales in the inertial range, but so does, simultaneously, nonlinear mode coupling, in a critically-balanced fashion. The net result is fast dissipation, but only at wavenumbers $k \gtrsim k_\nu \sim 1/\ell_\nu$ and $s \gtrsim s_\nu \sim 1/u_\nu$, which, by construction, satisfy the critical-balance condition (47). The nonlinear cascade ensures that all the injected δC_2 flux at large phase-space scales is rapidly dissipated at small scales via collisions, no matter how small is ν . This reduction of τ_ν is also an *a posteriori* justification of the assumption (25) of there being a separation of time scales between the time that it takes δC_2 to reach quasi-steady state and the time that it takes for the injection rate ε to decay due to the stochastic heating of $\langle f \rangle$ [87].

C. Implications and outlook

As discussed in Section VIB, these results provide a conceptual understanding of the role of phase mixing in turbulent plasmas. Recent theoretical [35, 61] and numerical [88, 89] studies have suggested a statistical ‘fluidization’ of turbulent, collisionless plasmas by stochastic plasma echoes suppressing phase mixing in the (spatial) inertial range. This might have seemed to be at odds with Landau damping [90] clearly being identified in turbulent settings numerically [84, 91–95] in several works, as well in Magnetospheric Multiscale (MMS) mission observations of the turbulent plasma in the Earth’s magnetosheath [96, 97]. While our model is quite simplified and does not include self-consistent electric fields and hence Landau damping, insofar as Landau damping and phase mixing are intimately related processes, our results indicate that these two seemingly contradictory sets of results can in fact be compatible.

This work also has implications for the relaxation of mean distribution functions in nearly collisionless plasmas. The existence of the entropy cascade implies that collisions will always dissipate fine-scale structure in the distribution function, even when ν is vanishingly small, but it does not necessarily imply that the rate by which the distribution function relaxes toward a Maxwellian is enhanced. This is clear in our model from the fact that, whereas δf develops sharp phase-space gradients, $\langle f \rangle$ does not, so Coulomb collisions are never activated for it. Mean distributions in space plasmas can be highly non-Maxwellian, e.g., in the solar wind [1, 6, 98]. Developing a theoretical formalism to predict the form of such non-equilibrium distribution functions is an outstanding problem. A direct consequence of entropy cascades is that theories of relaxation that assume phase-volume conservation [99–103] may not apply to nearly collisionless plasmas that are strongly turbulent. An alternative approach is to examine how the turbulent phase-space correlations of δf drive the evolution of the mean distribution function [43, 104].

There is much opportunity to understand phase-space entropy cascades in nearly collisionless plasmas better, with theory, numerical simulations, laboratory experiments, and spacecraft data. With regards to the latter two, the works [30, 105–107] suggest that measuring entropy cascades in real plasmas is a realizable endeavor just beginning to be possible.

M.L.N is grateful to I. Abel, T. Adkins, M. Allen, W. Clarke, S. Cowley, P. Dellar, J.-B. Fouvry, M. Kunz, R. Meyrand, F. Rincon, and J. Squire for helpful discussions related to this work. W.S would like to thank A. Bhattacharjee and H. Weitzner for useful discussions. We are also grateful to two anonymous referees, whose feedback improved the manuscript. M.L.N was supported by a Clarendon Scholarship. R.J.E was supported by a UK EPSRC studentship. W.S. was supported by a grant from the Simons Foundation/SFARI (560651, AB). The work of A.A.S. was supported in part by UK EPSRC (grant EP/R034737/1), STFC (grant ST/W000903/1), and the Simons Foundation via a Simons Investigator award. W.D.D. and M.L.N were supported by the US Department of Energy through grant DEFG0293ER54197 and Scientific Discovery Through Advanced Computing (SciDAC) grant UTA18000275.

Appendix A: Invariants alternative to C_2

In this appendix, we discuss invariants of the Vlasov equation alternative to C_2 . It is straightforward to show that (2) conserves an infinite number of invariants, so-called Casimir invariants [21]. Indeed, focusing on invariants defined in the averaged sense, for any smooth $g(f)$, the functional

$$G[f] = \frac{1}{L} \iint dx dv \langle g(f) \rangle \quad (\text{A1})$$

satisfies, using (7) for the collision operator,

$$\begin{aligned} \frac{dG}{dt} &= \frac{1}{L} \iint dx dv \langle g'(f) C[f] \rangle \\ &= -\frac{\nu}{L} \iint dx dv \left\langle g''(f) \left(\frac{\partial \langle f \rangle}{\partial v} + \frac{\partial \delta f}{\partial v} \right) \frac{\partial \delta f}{\partial v} \right\rangle \\ &\simeq -\frac{\nu}{L} \iint dx dv \left\langle g''(f) \left| \frac{\partial \delta f}{\partial v} \right|^2 \right\rangle, \end{aligned} \quad (\text{A2})$$

where the term with two derivatives on δf dominates when $\nu \rightarrow 0^+$. Note that while in this paper $\langle \dots \rangle$ denotes ensemble averaging with respect to the stochastic electric field, the arguments in this section hold for any averaging procedure for which one can decompose $f = \langle f \rangle + \delta f$, where $\langle \delta f \rangle = 0$.

When $\nu = 0$, every $G[f]$ is formally conserved. Furthermore, if $g(f)$ is convex, i.e., $g''(f) \geq 0$ everywhere, then the corresponding Casimirs are negative-definitely dissipated by collisions. We label Casimirs with positive-definite time evolution (which are minus the convex functionals of f) as ‘generalized entropies’ (cf. entropy functionals in hyperbolic partial differential equations [108]). This set includes $-C_2$, as well as the traditional entropy $S = -\iint dx dv f \log f$.

We define the relative entropy as

$$R[f] = G[f] - G[\langle f \rangle], \quad (\text{A3})$$

which has the budget

$$\frac{dR[f]}{dt} + \frac{dG[\langle f \rangle]}{dt} = -\frac{\nu}{L} \iint dx dv \left\langle g''(f) \left| \frac{\partial \delta f}{\partial v} \right|^2 \right\rangle. \quad (\text{A4})$$

Using (13), $G[\langle f \rangle]$ satisfies

$$\frac{dG[\langle f \rangle]}{dt} = -D_0 \int dv g''(\langle f \rangle) \left| \frac{\partial \langle f \rangle}{\partial v} \right|^2, \quad (\text{A5})$$

which is negative-definite if $g(f)$ is convex. Therefore, we can interpret (A4) analogously to (24). In the absence of collisions, as $G[\langle f \rangle]$ decreases via stochastic heating, $R[f]$ increases to maintain the $G[f]$ balance. Once δf has developed sharp enough gradients, collisions dissipate the total $G[f]$.

We have shown that C_2 is anomalously dissipated as $\nu \rightarrow 0^+$ and is cascaded, i.e., exhibits an inertial range unaffected directly by collisions or forcing. In principle, invariants other than C_2 can also have these properties. A system mathematically similar to (2) in which this happens is the advection-diffusion equation for a scalar advected by a turbulent flow: [109] showed that the family of invariants $\int d\mathbf{x} \theta^{2n}$, where θ is a scalar field and n is a positive integer, satisfy constant-flux cascades; in contrast, for a passive scalar advected by a smooth, chaotic flow (Batchelor regime), only the quadratic invariant ($n = 1$) is cascaded. This is because for higher-order invariants, logarithmic correlations of the passive

scalar give rise to injection of those invariants by the source at all scales, preventing the formation of an inertial range.

It is likely that a similar situation happens in the Vlasov-Kraichan model between the cases $\alpha < 2$ and $\alpha = 2$, but such a calculation is beyond the scope of this work. If it were true, then for $\alpha < 2$, the cascade of C_2 does not necessarily hold deeper physical meaning than the cascade of any other convex functional of f .

However, we still believe that C_2 is a particularly useful quantity in kinetic plasma turbulence. Because it is quadratic in f , C_2 is the only invariant (up to weight functions in the integrand of (A1)) that satisfies

$$G[\langle f \rangle + \delta f] = G[\langle f \rangle] + G[\delta f], \quad (\text{A6})$$

and so the relative entropy (A3) is a function solely of δf . This property is useful for conceptualizing the budget (A4) as a transfer of entropy between $\langle f \rangle$ and δf , as any other Casimir invariant involving higher powers of f will necessarily involve cross terms containing both $\langle f \rangle$ and δf . Furthermore, C_2 is the only invariant that lends itself to a simple Fourier analysis. For these reasons, in this paper, we have chosen to analyze phase-space turbulence using C_2 exclusively.

Appendix B: Derivation of the Fourier-spectrum equation

In this appendix, we give a detailed derivation of (33).

Multiplying (29) by $\delta \hat{f}^*(k, s)$, adding to the resulting equation its complex conjugate, and then ensemble averaging gives

$$\frac{\partial \hat{F}}{\partial t} + k \frac{\partial \hat{F}}{\partial s} + s \text{Im} \sum_p \left\langle \hat{E}(p) \delta \hat{f}(k-p) \delta \hat{f}^*(k) \right\rangle = \hat{S} - 2\nu s^2 \hat{F}. \quad (\text{B1})$$

Note that the second term in the Fourier sum in (29) vanishes under multiplication by $\delta \hat{f}^*(k, s)$ and ensemble averaging. The source term \hat{S} , defined in (34), comes from the second term on the right-hand side of (29). It can be found via application of the Furutsu-Novikov theorem (10) and using the fact that (3) implies

$$\langle \hat{E}(k, t) \hat{E}(k', t') \rangle = 2 \hat{D}(k) \delta_{k, -k'} \delta(t - t'), \quad (\text{B2})$$

where $\delta_{k, -k'}$ is the Kronecker delta.

1. Derivation of (32)

The δC_2 budget (32) in terms of \hat{F} can be found by taking the time derivative of (31) and using (B1). Assuming the spectrum goes to zero at $s \rightarrow \pm\infty$, the free-streaming term vanishes by integration over s . For the

nonlinear term, note that the summand in

$$\text{Im} \sum_{k,p} \left\langle \hat{E}(p) \delta \hat{f}(k-p, s) \delta \hat{f}^*(k, s) \right\rangle, \quad (\text{B3})$$

after taking $p \rightarrow -p$ and $k \rightarrow k-p$, and applying reality conditions on the electric field, is equal to its own complex conjugate. Therefore, its imaginary part vanishes. What is left is injection by the source and dissipation by collisions, viz., (32).

2. Derivation of (33)

We now close the triple correlator in (B1). Using (10), we have

$$\begin{aligned} \left\langle \hat{E}(p) \delta \hat{f}(k-p) \delta \hat{f}^*(k) \right\rangle &= \int dt' \sum_{p'} \left\langle \hat{E}(p, t) \hat{E}(p', t') \right\rangle \\ &\times \left\langle \frac{\delta \left[\delta \hat{f}(k-p, t) \delta \hat{f}^*(k, t) \right]}{\delta \hat{E}(p', t')} \right\rangle. \end{aligned} \quad (\text{B4})$$

As in Section II A, the functional derivative can be computed by formally integrating the relevant evolution equation. Using (29), we can write

$$\begin{aligned} &\delta \hat{f}(k-p) \delta \hat{f}^*(k) \\ &= \int^t dt'' \left\{ i s \sum_{p''} \left[\hat{E}(p'') \delta \hat{f}(k-p-p'') \delta \hat{f}^*(k) \right. \right. \\ &\quad \left. \left. - \hat{E}(-p'') \delta \hat{f}^*(k-p'') \delta \hat{f}(k-p) \right] + (\dots) \right\}, \end{aligned} \quad (\text{B5})$$

where (...) represents terms that will vanish after we take the functional derivative. Therefore, we get

$$\begin{aligned} &\left\langle \frac{\delta \left[\delta \hat{f}(k-p, t) \delta \hat{f}^*(k, t) \right]}{\delta \hat{E}(p', t')} \right\rangle \\ &= i s \left[\left\langle \delta \hat{f}(k-p-p', t') \delta \hat{f}^*(k, t') \right\rangle \right. \\ &\quad \left. - \left\langle \delta \hat{f}^*(k+p', t') \delta \hat{f}(k-p, t') \right\rangle \right] H(t-t'), \end{aligned} \quad (\text{B6})$$

where H is the Heaviside step function, defined with the convention that $H(0) = 1/2$. Combining this expression with (B2) and (B4) yields

$$\langle \hat{E}(p) \delta \hat{f}(k-p) \delta \hat{f}^*(k) \rangle = 2is \hat{D}(p) \left[\hat{F}(k) - \hat{F}(k-p) \right]. \quad (\text{B7})$$

Using this expression in (B1), we get

$$\begin{aligned} \frac{\partial \hat{F}}{\partial t} + k \frac{\partial \hat{F}}{\partial s} + 2s^2 \sum_p \hat{D}(p) \left[\hat{F}(k) - \hat{F}(k-p) \right] \\ = \hat{S} - 2\nu s^2 \hat{F}. \end{aligned} \quad (\text{B8})$$

3. The case of $\alpha = 2$: Batchelor limit

Let us simplify the nonlinear term in (B8) further. We start with the case of $\alpha = 2$. In the limit $kL_E \gg 1$, we suppose (and check *a posteriori*) that (5) is sufficiently steep in wavenumbers that we can consider $k \gg p$ and Taylor-expand the summand of the wavenumber sum in (B8):

$$\hat{F}(k) - \hat{F}(k-p) \simeq -p \frac{\partial \hat{F}}{\partial k} + \frac{1}{2} p^2 \frac{\partial^2 \hat{F}}{\partial k^2}. \quad (\text{B9})$$

This ‘Batchelor approximation’ was first used for the problem of passive-scalar mixing in fluids [65, 110] and amounts to approximating the electric field as effectively single-scale. Substituting (B9) back into the sum in (B8), the first term vanishes because it is odd in p , and we are left with

$$\sum_p \hat{D}(p) \left[\hat{F}(k) - \hat{F}(k-p) \right] \simeq D_2 \frac{\partial^2 \hat{F}}{\partial k^2}, \quad (\text{B10})$$

where

$$D_2 = \frac{1}{2} \sum_p p^2 \hat{D}(p) = \frac{D}{2} \sum_p \frac{p^2 e^{-(\eta p)^2}}{(p^2 + L_E^{-2})^{3/2}}. \quad (\text{B11})$$

In the limit $\eta \rightarrow 0^+$, (B11) is logarithmically divergent, being $\propto \log(L_E/\eta)$; without a small-scale cutoff, the approximation (B10) is invalid. This is because the k^{-3} spectrum in (5) is only marginally in the Batchelor regime [35, 65]. The Batchelor limit generically applies when the electric field is spatially smooth, corresponding to a rapidly decaying spectrum $\hat{D}(k)$. We choose the particular form of $\hat{D}(k)$ in (5) in order to match onto the Batchelor limit and fractional cases with one functional form of the correlation function, but we could just as well have picked a steeper (5) for $\alpha = 2$ that would not have required a small-scale cutoff. Therefore, without loss of generality, we keep (B11) without modification.

4. The $\alpha < 2$ cases: representation in terms of the fractional Laplacian

For $\alpha < 2$, it is convenient to manipulate the nonlinear term in (B8) in position space and then Fourier transform back to k space. We start by noting that

$$\begin{aligned} \sum_k e^{ikr} \sum_p \hat{D}(p) \left[\hat{F}(k) - \hat{F}(k-p) \right] \\ = [D(0) - D(r)] F(r). \end{aligned} \quad (\text{B12})$$

We now take the limits $\eta \rightarrow 0^+$ and $kL_E \gg 1$. When $\eta = 0$, note that (4) is the kernel of the Bessel potential [64, 111], and can therefore be written as

$$D(r) = \frac{LD}{2\pi} \frac{2^{1-\alpha/2} \sqrt{\pi} L_E^\alpha}{\Gamma(\frac{\alpha+1}{2})} \left(\frac{r}{L_E} \right)^{\alpha/2} K_{\alpha/2} \left(\frac{r}{L_E} \right), \quad (\text{B13})$$

where K is the modified Bessel function of the second kind, and Γ is the Gamma function. For $\alpha < 2$ and $r/L_E \ll 1$, (B13) has a series expansion

$$D(r) = D_0 - D_\alpha r^\alpha + \mathcal{O}\left(\frac{r^2}{L_E^{2-\alpha}}\right), \quad (\text{B14})$$

where

$$D_0 = \frac{LD}{2\pi} \frac{\Gamma(\frac{\alpha}{2}) \sqrt{\pi}}{\Gamma(\frac{\alpha+1}{2})} L_E^\alpha, \quad (\text{B15})$$

$$D_\alpha = \frac{LD}{2\pi} \frac{\sqrt{\pi} \left| \Gamma(\frac{-\alpha}{2}) \right|}{2^\alpha \Gamma(\frac{\alpha+1}{2})}. \quad (\text{B16})$$

We now Fourier transform back to k space. To lowest order in $(r/L_E)^{2-\alpha} \ll 1$ (equivalently, $(kL_E)^{2-\alpha} \gg 1$), the r^α term is dominant over the r^2 term, which gives

$$\begin{aligned} \frac{1}{L} \int dr e^{-ikr} [D(0) - D(r)] F(r) \\ \simeq \frac{1}{L} \int dr e^{-ikr} D_\alpha |r|^\alpha F(r) = D_\alpha (-\Delta_k)^{\alpha/2} \hat{F}(k). \end{aligned} \quad (\text{B17})$$

Here $(-\Delta_k)^{\alpha/2}$ is a fractional Laplacian [52–54] of order $\alpha/2$, in k space, viz.,

$$(-\Delta_k)^{\alpha/2} \hat{F}(k) = c_\alpha \text{p.v.} \int_{-\infty}^{+\infty} dp \frac{\hat{F}(k) - \hat{F}(k-p)}{|p|^{\alpha+1}}, \quad (\text{B18})$$

where

$$c_\alpha = \frac{2^\alpha \Gamma(\frac{\alpha+1}{2})}{\sqrt{\pi} \left| \Gamma(\frac{-\alpha}{2}) \right|}, \quad (\text{B19})$$

and p.v. means that the integral is defined in the principal-value sense.

Thus, using (B17) and (B10), we have that (B8) becomes (33), where

$$\kappa = \begin{cases} 2D_\alpha, & \alpha < 2, \\ 2D_2, & \alpha = 2, \end{cases} \quad (\text{B20})$$

with D_α given by (B16) and D_2 given by (B11).

5. Derivation of (105)

Here, we derive the form (105) of the non-local k flux in the $\alpha < 2$ cases, as analyzed in Section V D.

We first rewrite (B18) as an integral over positive p :

$$\begin{aligned} (-\Delta_k)^{\alpha/2} \hat{F}(k) &= c_\alpha \text{p.v.} \int_{-\infty}^{+\infty} dp \frac{\hat{F}(k) - \hat{F}(k-p)}{|p|^{\alpha+1}} \\ &= c_\alpha \int_0^\infty dp \frac{2\hat{F}(k) - \hat{F}(k-p) - \hat{F}(k+p)}{p^{\alpha+1}}. \end{aligned} \quad (\text{B21})$$

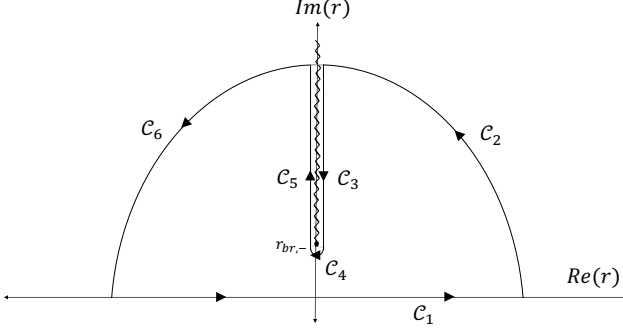


FIG. 6. Contour used in the derivation of (65).

In (B21), we can write $p^{-(\alpha+1)} = -(1/\alpha)\partial_p p^{-\alpha}$ and integrate by parts. The boundary terms vanish (assuming \hat{F} vanishes at infinity), and we are left with

$$\begin{aligned} (-\Delta_k)^{\alpha/2} \hat{F}(k) &= -\frac{c_\alpha}{\alpha} \int_0^\infty dp \frac{\frac{\partial \hat{F}}{\partial p}(k-p) + \frac{\partial \hat{F}}{\partial p}(k+p)}{p^\alpha} \\ &= \frac{\partial}{\partial k} \frac{c_\alpha}{\alpha} \int_0^\infty dp \frac{\hat{F}(k-p) - \hat{F}(k+p)}{p^\alpha}. \end{aligned} \quad (\text{B22})$$

Combining (B22) and the definition $\partial_k \hat{\Gamma}^k = \kappa s^2 (-\Delta_k)^{\alpha/2} \hat{F}$ yields (105).

Appendix C: Detailed calculations for Section IV A

In this appendix, we derive the general $\alpha < 2$ expressions for $\hat{g}(k)$ (65) and the k flux integrated over s (69).

1. Derivation of (65) and (72)

We start with $\hat{g}(k)$, as given in (62). As discussed in Section IV A, it is useful to convert this integral into one where the exponential in the integrand is decaying rather than oscillatory. To do this, we perform an auxiliary expansion, taking $|r|^\alpha \rightarrow (r^2 + \delta^2)^{\alpha/2}$ and then $\delta \rightarrow 0$ in the integral (62):

$$\hat{g}(k) = \frac{\varepsilon}{2\pi\kappa L} \lim_{\delta \rightarrow 0} \mathcal{I}_{C_1}, \quad (\text{C1})$$

where

$$\mathcal{I}_{C_1} = \int_{C_1} dr \frac{e^{-ikr}}{(r^2 + \delta^2)^{\alpha/2} + \ell_\nu^\alpha}, \quad (\text{C2})$$

and C_1 is a contour running along the real line. We choose the branch cuts so that

$$\begin{aligned} (r^2 + \delta^2)^{\alpha/2} &= (r + i\delta)^{\alpha/2} (r - i\delta)^{\alpha/2} \\ &= r_+^{\alpha/2} e^{i\alpha\theta_+/2} r_-^{\alpha/2} e^{i\alpha\theta_-/2}, \end{aligned} \quad (\text{C3})$$

where $r_\pm = |r \pm i\delta|$, $\theta_+ \in [-\pi/2, 3\pi/2]$, and $\theta_- \in [-3\pi/2, \pi/2]$. Note the branch points are at $r_{\text{br},\pm} = \mp i\delta$. We first treat the case $k < 0$. We close C_1 by making a semi-circle in the upper half of the complex plane and going around the branch cut with the branch point $r_{\text{br},-}$, as depicted in Fig. 6. By Cauchy's residue theorem, since the integrand in (C2) has no poles, $\mathcal{I}_{C_1} + \mathcal{I}_{C_2} + \mathcal{I}_{C_3} + \mathcal{I}_{C_4} + \mathcal{I}_{C_5} + \mathcal{I}_{C_6} = 0$. When the radius R of the contours C_2 and C_6 is large, the integrands along these contours are $\propto e^{-|k|R \sin \theta} R^{1-\alpha}$ (here θ is the angle of the contour with respect to the positive real axis). Thus, \mathcal{I}_{C_2} and \mathcal{I}_{C_6} tend to zero as $R \rightarrow \infty$. Because the integrand is finite at $r = r_{\text{br},-}$, \mathcal{I}_{C_4} tends to zero as the radius of C_4 shrinks to zero. Therefore, $\mathcal{I}_{C_1} = -\mathcal{I}_{C_3} - \mathcal{I}_{C_5}$. Noting that along C_3 , $\theta_\pm = \pi/2$, while along C_5 , $\theta_+ = \pi/2$ and $\theta_- = -3\pi/2$, we have that

$$\begin{aligned} -(\mathcal{I}_{C_3} + \mathcal{I}_{C_5}) &= -i \int_\infty^\delta dz \frac{e^{-|k|z}}{(z^2 - \delta^2)^{\alpha/2} e^{i\pi\alpha/2} + \ell_\nu^\alpha} \\ &= -i \int_\delta^\infty dz \frac{e^{-|k|z}}{(z^2 - \delta^2)^{\alpha/2} e^{-i\pi\alpha/2} + \ell_\nu^\alpha} \\ &= 2 \int_\delta^\infty dz e^{-|k|z} \\ &\quad \times \frac{\sin(\pi\alpha/2)(z^2 - \delta^2)^{\alpha/2}}{(z^2 - \delta^2)^\alpha + 2(z^2 - \delta^2)^{\alpha/2} \ell_\nu^\alpha \cos(\pi\alpha/2) + \ell_\nu^{2\alpha}}, \end{aligned} \quad (\text{C4})$$

where we have changed variables to $z = -ir$ and used the fact that $\mathcal{I}_{C_5} = \mathcal{I}_{C_3}^*$. Now we can safely take the limit $\delta \rightarrow 0$. Using Cauchy's residue theorem and also redefining $z \rightarrow \ell_\nu z$, we have

$$\begin{aligned} \hat{g}(k) &= \frac{\varepsilon}{2\pi\kappa L} \lim_{\delta \rightarrow 0} \mathcal{I}_{C_1} = \frac{\varepsilon}{2\pi\kappa L} \lim_{\delta \rightarrow 0} \left[-(\mathcal{I}_{C_3} + \mathcal{I}_{C_5}) \right] \\ &= \frac{\varepsilon \ell_\nu}{2\pi\nu L} \int_0^\infty dz \frac{\sin(\pi\alpha/2) z^\alpha}{z^{2\alpha} + 2z^\alpha \cos(\pi\alpha/2) + 1} e^{-|k|\ell_\nu z}, \end{aligned} \quad (\text{C5})$$

which is (65). For $k > 0$, C_1 can be closed by making a contour in the lower half plane, yielding the same expression (C5). Integrating this expression in k and multiplying by $2\nu L$ immediately yields (72).

2. Derivation of (69)

For the k flux, combining (61) and (67), we have

$$L \int ds \hat{\Gamma}^k = \frac{i\varepsilon}{2\pi} \int dr \frac{|r|^\alpha}{r} \frac{e^{-ikr}}{|r|^\alpha + \ell_\nu^\alpha}. \quad (\text{C6})$$

This integral can be equated to one where the exponential term is decaying rather than oscillatory by again substituting $|r|^\alpha \rightarrow (r^2 + \delta^2)^{\alpha/2}$ and then taking $\delta \rightarrow 0$. The method from Appendix C 1 can be applied again, resulting in (69). The main difference is that this time, the auxiliary expansion in δ introduces a pole at $r = 0$ in the integrand of (C6), making it necessary to deform the

contour along the real line. However, this residue contribution vanishes when $\delta \rightarrow 0$, so whether the contour is deformed below or above the pole does not change the final answer.

Given the expression (69), we can take its asymptotics for $k\ell_\nu \ll 1$, as analyzed in Section IV A. In this limit, the inertial-range flux is approximately equal to the rate of δC_2 injection. Changing variables to $u = z^\alpha$, we have

$$\begin{aligned} & L \int ds \hat{\Gamma}^k \\ & \simeq \text{sgn}(k) \frac{\varepsilon \sin(\pi\alpha/2)}{\pi\alpha} \int_0^\infty \frac{du}{u^2 + 2u \cos(\pi\alpha/2) + 1} \\ & = \text{sgn}(k) \frac{\varepsilon \sin(\pi\alpha/2)}{\pi\alpha} \frac{1}{\sin(\pi\alpha/2)} \frac{\pi\alpha}{2} \\ & = \text{sgn}(k) \frac{\varepsilon}{2}, \end{aligned} \quad (\text{C7})$$

where the u integral was done using [112], formula 3.252(1). Note this result also implies that (72) approximately satisfies $\hat{D}(k) \simeq \varepsilon$ when $k\ell_\nu \gg 1$.

3. Expressions for $\alpha = 1$ case

Finally, we note that when $\alpha = 1$, $\hat{g}(k)$, $\hat{D}(k)$, and $L \int ds \hat{\Gamma}^k$ can all be expressed in terms of known special functions. For the sake of completeness, we give these expressions here.

For $\hat{g}(k)$, using [74], formulas 5.2.7 and 5.2.13, we have

$$\begin{aligned} \hat{g}(k) &= \frac{\varepsilon \ell_\nu}{2\pi\nu L} \int_0^\infty dz \frac{z e^{-|k|\ell_\nu z}}{z^2 + 1} \\ &= -\frac{\varepsilon \ell_\nu}{2\pi\nu L} [\cos(|k|\ell_\nu) \text{Ci}(|k|\ell_\nu) + \sin(|k|\ell_\nu) \text{si}(|k|\ell_\nu)], \end{aligned} \quad (\text{C8})$$

where $\text{Ci}(z)$ and $\text{si}(z)$ are cosine and sine integral functions [74], respectively.

For $\hat{D}(k)$, using [74], formulas 5.2.6 and 5.2.12, we have

$$\begin{aligned} \hat{D}(k) &= \frac{2\varepsilon}{\pi} \int_0^\infty dz \frac{1 - e^{-k\ell_\nu z}}{z^2 + 1} \\ &= \varepsilon \left\{ 1 - \frac{2}{\pi} [\sin(k\ell_\nu) \text{Ci}(k\ell_\nu) - \cos(k\ell_\nu) \text{si}(k\ell_\nu)] \right\}. \end{aligned} \quad (\text{C9})$$

When $k\ell_\nu \ll 1$, (C9) has the series

$$\hat{D}(k) = \varepsilon \left\{ \frac{2}{\pi} [1 - \gamma - \log(k\ell_\nu)] k\ell_\nu + \mathcal{O}((k\ell_\nu)^2) \right\}, \quad (\text{C10})$$

which vanishes as $k\ell_\nu \rightarrow 0$. Here, γ is the Euler–Mascheroni constant. Note that the finite- $k\ell_\nu$ corrections are linear and logarithmic, in contrast to the $\alpha = 2$ case (71), where the first-order correction (after

Taylor expanding the exponential) is just linear in $k\ell_\nu$. When $k\ell_\nu \gg 1$, (C9) has the series

$$\hat{D}(k) = \varepsilon \left[1 - \frac{2}{\pi} \frac{1}{k\ell_\nu} + \mathcal{O}((k\ell_\nu)^{-3}) \right]. \quad (\text{C11})$$

Likewise, the integrated k flux (69) is

$$\begin{aligned} L \int ds \hat{\Gamma}^k &= \text{sgn}(k) \frac{\varepsilon}{\pi} \int_0^\infty dz \frac{e^{-|k|\ell_\nu z}}{z^2 + 1} \\ &= \text{sgn}(k) \frac{\varepsilon}{\pi} [\sin(|k|\ell_\nu) \text{Ci}(|k|\ell_\nu) - \cos(|k|\ell_\nu) \text{si}(|k|\ell_\nu)]. \end{aligned} \quad (\text{C12})$$

When $k\ell_\nu \ll 1$, this expression has the series

$$\begin{aligned} L \int ds \hat{\Gamma}^k &= \text{sgn}(k) \frac{\varepsilon}{2} \left\{ 1 - \frac{2}{\pi} [1 - \gamma - \log(|k|\ell_\nu)] |k|\ell_\nu \right. \\ & \quad \left. + \mathcal{O}((|k|\ell_\nu)^2) \right\}, \end{aligned} \quad (\text{C13})$$

in agreement with (C7) as $k\ell_\nu \rightarrow 0$.

Appendix D: Closed-form expressions of inertial-range spectrum and fluxes for $\alpha = 1$

In Sections VB and VC, we plotted the inertial-range spectrum and its corresponding vector flux, respectively, for $\alpha = 1$. For this value of α , the spectrum and fluxes have simple closed forms, which we derive in this appendix.

When $\alpha = 1$, (87) reduces to

$$\phi(y) = \tilde{\sigma} e^{-(1-i)y/\sqrt{3}}, \quad (\text{D1})$$

where we have absorbed all order-unity constants into $\tilde{\sigma}$, where $\tilde{\sigma} = 3^{1/4} 2^{-3/4} \sqrt{\pi} \sigma$. In (89), therefore, we have

$$\begin{aligned} & 2 \text{Re} \int_0^\infty dy e^{-i\xi y} \phi(y) \\ &= 2\tilde{\sigma} \text{Re} \int_0^\infty dy e^{-y/\sqrt{3}} e^{-iy(\xi-1/\sqrt{3})} \\ &= 2\sqrt{3} \tilde{\sigma} \frac{1}{3\xi^2 - 2\sqrt{3}\xi + 2}. \end{aligned} \quad (\text{D2})$$

The constant $\tilde{\sigma}$ can be found via the flux constraint (82):

$$\begin{aligned} \frac{1}{2} &= 2\sqrt{3} \tilde{\sigma} \int_{-\infty}^{+\infty} d\xi \frac{\xi}{3\xi^2 - 2\sqrt{3}\xi + 2} = 2\sqrt{3} \tilde{\sigma} \frac{\pi}{3} \\ \implies \tilde{\sigma} &= \frac{\sqrt{3}}{4\pi}. \end{aligned} \quad (\text{D3})$$

Therefore, using (83) and (89), the spectrum is

$$\begin{aligned} \hat{F}(k, s) &= \frac{3\varepsilon}{2\pi L \kappa} s^{-3} \frac{1}{3\xi^2 - 2\sqrt{3}\xi + 2} \\ &= \frac{3\varepsilon}{2\pi L} \frac{1}{3k^2 - 2\sqrt{3}\kappa k s^{3/2} + 2\kappa s^3}. \end{aligned} \quad (\text{D4})$$

This expression clearly satisfies the asymptotics given by (54), and the results for the 1-D spectra (48) and (51) apply.

The s flux (56) is then simply

$$\hat{\Gamma}^s = k\hat{F} = \frac{3\varepsilon}{2\pi L} \frac{k}{3k^2 - 2\sqrt{3\kappa}ks^{3/2} + 2\kappa s^3}. \quad (\text{D5})$$

The k flux (57), using (95), is

$$\begin{aligned} \hat{\Gamma}^k &= -2\varepsilon L^{-1}s^{-1} \text{Im} \int_0^\infty dy e^{-i\xi y} \phi(y). \\ &= -\frac{\sqrt{3}\varepsilon}{2\pi Ls} \text{Im} \int_0^\infty dy e^{-y/\sqrt{3}} e^{-iy(\xi-1/\sqrt{3})} \\ &= \frac{3\varepsilon}{2\pi Ls} \frac{\sqrt{3}\xi - 1}{3\xi^2 - 2\sqrt{3}\xi + 2} \\ &= \frac{3\varepsilon}{2\pi L} \frac{\sqrt{3\kappa}ks^{1/2} - \kappa s^2}{3k^2 - 2\sqrt{3\kappa}ks^{3/2} + 2\kappa s^3}. \end{aligned} \quad (\text{D6})$$

Finally, we show that the components of the shell-averaged flux (107) for $\alpha = 1$ are positive-definite. For the s flux, using (D5) and (107), we have

$$\begin{aligned} \hat{\Gamma}^s(k, s) + \hat{\Gamma}^s(-k, s) &= \frac{3\varepsilon k}{2\pi L\kappa s^3} \left(\frac{1}{3\xi^2 - 2\sqrt{3}\xi + 2} - \frac{1}{3\xi^2 + 2\sqrt{3}\xi + 2} \right) \\ &= \frac{3\varepsilon k}{2\pi L\kappa s^3} \frac{4\sqrt{3}\xi}{9\xi^4 + 4} \geq 0. \end{aligned} \quad (\text{D7})$$

For the k flux, using (D6) and (107), we have

$$\begin{aligned} \hat{\Gamma}^k(k, s) - \hat{\Gamma}^k(-k, s) &= \frac{3\varepsilon}{2\pi Ls} \left(\frac{\sqrt{3}\xi - 1}{3\xi^2 - 2\sqrt{3}\xi + 2} + \frac{\sqrt{3}\xi + 1}{3\xi^2 + 2\sqrt{3}\xi + 2} \right) \\ &= \frac{3\varepsilon}{2\pi Ls} \frac{6\sqrt{3}\xi^3}{9\xi^4 + 4} \geq 0. \end{aligned} \quad (\text{D8})$$

Appendix E: Characterization of 2-D fluxes for $\alpha < 2$ cases

In this section, we characterize the (non-local) 2-D fluxes for the $\alpha < 2$ cases. The asymptotics of the (normalized) ratio of fluxes (106) are

$$R \sim \begin{cases} -(kL_0)^{-1} (sv_{\text{th}})^{(5-\alpha)/(\alpha+1)}, & \xi \ll 1, \\ (kL_0)^{1-\alpha} (sv_{\text{th}})^{(2\alpha-1)/(\alpha+1)}, & \xi \gg 1. \end{cases} \quad (\text{E1})$$

Unlike in the Batchelor regime, the ratios in (E1) are no longer functions solely of ξ , and, therefore, the regions where R is small or large are not necessarily divided by the critical-balance curve (47). Note that we focus our analysis on the top right quadrant of the (k, s) plane, but our arguments can be extended to the whole plane.

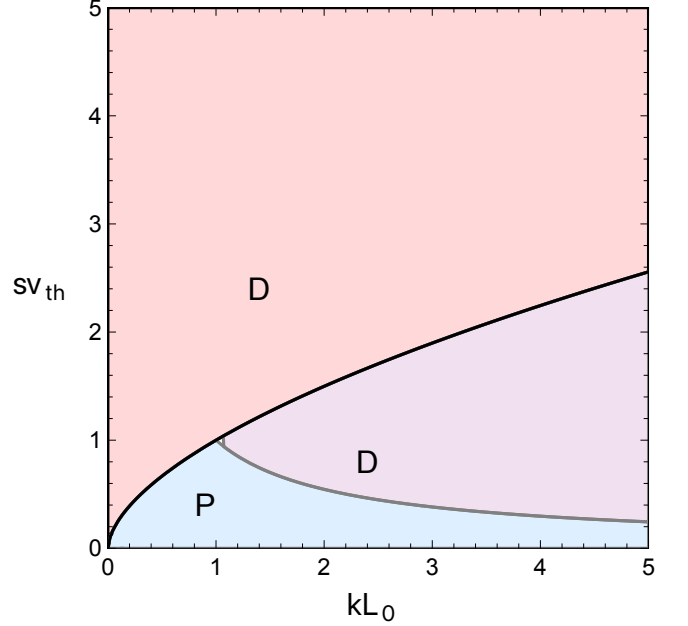


FIG. 7. Cartoon diagram depicting the regions where the flux is phase-mixing-dominated (labeled ‘P’ and colored blue) versus diffusion-dominated (labeled ‘D’ and colored red), for $\alpha = 3/4$. The black curve is the critical-balance curve (47) for this value of α , $sv_{\text{th}} \sim (kL_0)^{7/12}$. The gray curve is (E3) for these parameters, $sv_{\text{th}} \sim (kL_0)^{-7/8}$. We have colored the region bounded above by the critical-balance curve and below by (E3) as purple to emphasize that it is still a region where phase mixing is locally dominant, viz., (42) is large, despite the flux being diffusion-dominated there.

For $\xi \ll 1$, above the curve (47), which is the diffusion-dominated region for $\alpha = 2$, the s and k flux are comparable along the curve

$$sv_{\text{th}} \sim (kL_0)^{(\alpha+1)/(5-\alpha)}. \quad (\text{E2})$$

At sufficiently large kL_0 , this curve falls below the critical-balance curve (47), outside the $\xi \ll 1$ regime, and hence $\hat{\Gamma}^k$ is dominant over $\hat{\Gamma}^s$ when $\xi \ll 1$ for all α .

For $\xi \gg 1$, below the curve (47), which is the phase-mixing-dominated region for $\alpha = 2$, the s and k flux are comparable along the curve

$$sv_{\text{th}} \sim (kL_0)^{(\alpha^2-1)/(2\alpha-1)}. \quad (\text{E3})$$

There are now various regimes with different behaviors. When $1 < \alpha < 2$, the flux is phase-mixing-dominated (diffusion-dominated) below (above) the curve (E3). At sufficiently large kL_0 , the curve (E3) falls below the critical-balance curve (47), effectively widening the diffusion-dominated region from the $\xi \ll 1$ region down to the curve (E3). Note that for this range of α , (E3) is concave, same as (47).

When $\alpha = 1$, (E3) is horizontal in kL_0 , and so the flux is only phase-mixing-dominated for $sv_{\text{th}} \ll 1$, irrespective of k . We plotted this case in Fig. 4(b).

When $1/2 < \alpha < 1$, sv_{th} in (E3) is a decreasing function of kL_0 , shrinking the phase-mixing-dominated region further. As an example, we plot a diagram for the case $\alpha = 3/4$ in Fig. 7. Note that when $\alpha < -1 + \sqrt{3} \simeq 0.732$, the dependence of sv_{th} on kL_0 in (E3) is steeper than $(kL_0)^{-1}$, so the area of the phase-mixing-dominated region becomes finite.

When $\alpha = 1/2$, the flux is phase-mixing-dominated only when $kL_0 \ll 1$, irrespective of s . Note that k must satisfy $kL_E \gg 1$ to be in the inertial range (and $\xi \gg 1$ for these asymptotics to hold), so the phase-mixing-

dominated region is likely nonexistent.

When $0 < \alpha < 1/2$, the curve (E3) is convex. The phase-mixing-dominated region is bounded below by (E3) and above by (47), extending from $k = 0$ to the intersection of (E3) and (47), viz., at $kL_0 = 1$. The region where the flux is phase-mixing-dominated is not asymptotic, i.e., everywhere in the $\xi \gg 1$ region, in the limit $\xi \rightarrow \infty$, either in the limit $kL_0 \rightarrow \infty$ and/or $sv_{\text{th}} \rightarrow 0$, the flux is diffusion-dominated. Therefore, in this case, the only part of the (k, s) plane where the flux is phase-mixing dominated is along the curve $\xi = \xi_\alpha$, where the k flux vanishes.

-
- [1] E. Marsch, Kinetic physics of the solar corona and solar wind, *Living Reviews in Solar Physics* **3**, 1 (2006).
- [2] A. A. Schekochihin, S. C. Cowley, W. Dorland, G. W. Hammett, G. G. Howes, E. Quataert, and T. Tatsuno, Astrophysical gyrokinetics: kinetic and fluid turbulent cascades in magnetized weakly collisional plasmas, *Astrophysical Journal Supplement Series* **182**, 310 (2009).
- [3] G. Zimbardo, A. Greco, L. Sorriso-Valvo, S. Perri, Z. Vörös, G. Aburjania, K. Chargazia, and O. Alexandrova, Magnetic turbulence in the geospace environment, *Space Science Reviews* **156**, 89 (2010).
- [4] C. Chen, Recent progress in astrophysical plasma turbulence from solar wind observations, *Journal of Plasma Physics* **82**, 535820602 (2016).
- [5] G. G. Howes, A prospectus on kinetic heliophysics, *Physics of Plasmas* **24**, 055907 (2017).
- [6] D. Verscharen, K. G. Klein, and B. A. Maruca, The multi-scale nature of the solar wind, *Living Reviews in Solar Physics* **16**, 5 (2019).
- [7] S. R. Cranmer and A. R. Winebarger, The properties of the solar corona and its connection to the solar wind, *Annual Review of Astronomy and Astrophysics* **57**, 157 (2019).
- [8] E. Quataert and A. Gruzinov, Turbulence and particle heating in advection-dominated accretion flows, *Astrophysical Journal* **520**, 248 (1999).
- [9] A. Chael, M. Rowan, R. Narayan, M. Johnson, and L. Sironi, The role of electron heating physics in images and variability of the galactic centre black hole Sagittarius A*, *Monthly Notices of the Royal Astronomical Society* **478**, 5209 (2018).
- [10] K. Akiyama, A. Alberdi, W. Alef, K. Asada, R. Azulay, A.-K. Bacsko, D. Ball, M. Baloković, J. Barrett, D. Bintley, *et al.*, First M87 Event Horizon Telescope results. V. Physical origin of the asymmetric ring, *Astrophysical Journal Letters* **875**, L5 (2019).
- [11] L. Boltzmann, *Vorlesungen über Gastheorie* (J. A. Barth, Leipzig, 1896).
- [12] L. D. Landau, The transport equation in the case of Coulomb interactions, in *Collected Papers of L.D. Landau*, edited by D. ter Haar (Pergamon Press, Oxford, 1965) pp. 163–170.
- [13] T. N. Parashar, C. Salem, R. T. Wicks, H. Karimabadi, S. P. Gary, and W. H. Matthaeus, Turbulent dissipation challenge: a community-driven effort, *Journal of Plasma Physics* **81**, 905810513 (2015).
- [14] W. H. Matthaeus, Y. Yang, M. Wan, T. N. Parashar, R. Bandyopadhyay, A. Chasapis, O. Pezzi, and F. Valentini, Pathways to dissipation in weakly collisional plasmas, *Astrophysical Journal* **891**, 101 (2020).
- [15] S. Roy, R. Bandyopadhyay, Y. Yang, T. Parashar, W. Matthaeus, S. Adhikari, V. Roytershteyn, A. Chasapis, H. Li, D. Gershman, *et al.*, Turbulent energy transfer and proton–electron heating in collisionless plasmas, *Astrophysical Journal* **941**, 137 (2022).
- [16] R. Marino and L. Sorriso-Valvo, Scaling laws for the energy transfer in space plasma turbulence, *Physics Reports* **1006**, 1 (2023).
- [17] J. Birn, J. Drake, M. Shay, B. Rogers, R. Denton, M. Hesse, M. Kuznetsova, Z. Ma, A. Bhattacharjee, A. Otto, *et al.*, Geospace environmental modeling (GEM) magnetic reconnection challenge, *Journal of Geophysical Research: Space Physics* **106**, 3715 (2001).
- [18] M. Yamada, R. Kulsrud, and H. Ji, Magnetic reconnection, *Reviews of Modern Physics* **82**, 603 (2010).
- [19] A. Lazarian, G. L. Eyink, A. Jafari, G. Kowal, H. Li, S. Xu, and E. T. Vishniac, 3D turbulent reconnection: theory, tests, and astrophysical implications, *Physics of Plasmas* **27**, 012305 (2020).
- [20] H. Ji, W. Daughton, J. Jara-Almonte, A. Le, A. Stanier, and J. Yoo, Magnetic reconnection in the era of exascale computing and multiscale experiments, *Nature Reviews Physics* **4**, 263 (2022).
- [21] H. Ye and P. J. Morrison, Action principles for the Vlasov equation, *Physics of Fluids B* **4**, 771 (1992).
- [22] J. A. Krommes and G. Hu, The role of dissipation in the theory and simulations of homogeneous plasma turbulence, and resolution of the entropy paradox, *Physics of Plasmas* **1**, 3211 (1994).
- [23] J. A. Krommes, Thermostatted δf , *Physics of Plasmas* **6**, 1477 (1999).
- [24] A. A. Schekochihin, S. C. Cowley, W. Dorland, G. W. Hammett, G. G. Howes, G. G. Plunk, E. Quataert, and T. Tatsuno, Gyrokinetic turbulence: a nonlinear route to dissipation through phase space, *Plasma Physics and Controlled Fusion* **50**, 124024 (2008).
- [25] T. Tatsuno, W. Dorland, A. A. Schekochihin, G. G. Plunk, M. Barnes, S. C. Cowley, and G. G. Howes, Nonlinear phase mixing and phase-space cascade of entropy in gyrokinetic plasma turbulence, *Physical Review Letters* **103**, 015003 (2009).
- [26] G. G. Plunk, S. C. Cowley, A. A. Schekochihin, and

- T. Tatsuno, Two-dimensional gyrokinetic turbulence, *Journal of Fluid Mechanics* **664**, 407 (2010).
- [27] W. Dorland and G. Hammett, Gyrofluid turbulence models with kinetic effects, *Physics of Fluids B: Plasma Physics* **5**, 812 (1993).
- [28] U. Frisch, *Turbulence: The Legacy of A. N. Kolmogorov* (Cambridge University Press, Cambridge, 1995).
- [29] G. L. Eyink and K. R. Sreenivasan, Onsager and the theory of hydrodynamic turbulence, *Reviews of Modern Physics* **78**, 87 (2006).
- [30] S. Servidio, A. Chasapis, W. H. Matthaeus, D. Perrone, F. Valentini, T. N. Parashar, P. Veltri, D. Gershman, C. T. Russell, B. Giles, S. A. Fuselier, T. D. Phan, and J. Burch, Magnetospheric Multiscale observation of plasma velocity-space cascade: Hermite representation and theory, *Physical Review Letters* **119**, 205101 (2017).
- [31] S. Cerri, M. W. Kunz, and F. Califano, Dual phase-space cascades in 3D hybrid-Vlasov–Maxwell turbulence, *Astrophysical Journal Letters* **856**, L13 (2018).
- [32] O. Pezzi, S. Servidio, D. Perrone, F. Valentini, L. Sorriso-Valvo, A. Greco, W. Matthaeus, and P. Veltri, Velocity-space cascade in magnetized plasmas: numerical simulations, *Physics of Plasmas* **25**, 060704 (2018).
- [33] G. L. Eyink, Cascades and dissipative anomalies in nearly collisionless plasma turbulence, *Physical Review X* **8**, 041020 (2018).
- [34] G. Celebre, S. Servidio, and F. Valentini, Phase space dynamics of unmagnetized plasmas: Collisionless and collisional regimes, *Physics of Plasmas* **30**, 092304 (2023).
- [35] T. Adkins and A. A. Schekochihin, A solvable model of Vlasov-kinetic plasma turbulence in Fourier–Hermite phase space, *Journal of Plasma Physics* **84**, 905840107 (2018).
- [36] R. H. Kraichnan, Small-scale structure of a scalar field convected by turbulence, *Physics of Fluids* **11**, 945 (1968).
- [37] Or a vector field, such as a magnetic field, in which case the model is named after Kazantsev, who, in the year before Kraichnan, pursued the same type of approximation for the kinematic-dynamo problem [113, 114].
- [38] G. Eyink and U. Frisch, “Robert H. Kraichnan”, in *A Voyage Through Turbulence*, edited by P. A. Davidson, Y. Kaneda, K. Moffatt, and K. R. Sreenivasan (Cambridge University Press, Cambridge, 2011) p. 329–372.
- [39] G. Falkovich, K. Gawedzki, and M. Vergassola, Particles and fields in fluid turbulence, *Reviews of Modern Physics* **73**, 913 (2001).
- [40] P. A. Sturrock, Stochastic acceleration, *Physical Review* **141**, 186 (1966).
- [41] B. D. Chandran, B. Li, B. N. Rogers, E. Quataert, and K. Germaschewski, Perpendicular ion heating by low-frequency Alfvén-wave turbulence in the solar wind, *Astrophysical Journal* **720**, 503 (2010).
- [42] S. S. Cerri, L. Arzamasskiy, and M. W. Kunz, On stochastic heating and its phase-space signatures in low-beta kinetic turbulence, *Astrophysical Journal* **916**, 120 (2021).
- [43] P. H. Diamond, S.-I. Itoh, and K. Itoh, *Modern Plasma Physics: Volume 1, Physical Kinetics of Turbulent Plasmas* (Cambridge University Press, Cambridge, 2010).
- [44] Y. Kosuga and P. Diamond, On relaxation and transport in gyrokinetic drift wave turbulence with zonal flow, *Physics of Plasmas* **18**, 122305 (2011).
- [45] M. Lesur and P. H. Diamond, Nonlinear instabilities driven by coherent phase-space structures, *Physical Review E* **87**, 031101(R) (2013).
- [46] V. Zhdankin, Generalized entropy production in collisionless plasma flows and turbulence, *Physical Review X* **12**, 031011 (2022).
- [47] V. Zhdankin, Non-thermal particle acceleration from maximum entropy in collisionless plasmas, *Journal of Plasma Physics* **88**, 175880303 (2022).
- [48] K. Hallatschek, Thermodynamic potential in local turbulence simulations, *Physical Review Letters* **93**, 125001 (2004).
- [49] I. G. Abel, G. G. Plunk, E. Wang, M. Barnes, S. C. Cowley, W. Dorland, and A. A. Schekochihin, Multi-scale gyrokinetics for rotating tokamak plasmas: fluctuations, transport and energy flows, *Reports on Progress in Physics* **76**, 116201 (2013).
- [50] A. Zocco and A. A. Schekochihin, Reduced fluid-kinetic equations for low-frequency dynamics, magnetic reconnection, and electron heating in low-beta plasmas, *Physics of Plasmas* **18**, 102309 (2011).
- [51] A. Kanekar, A. A. Schekochihin, W. Dorland, and N. F. Loureiro, Fluctuation-dissipation relations for a plasma-kinetic Langevin equation, *Journal of Plasma Physics* **81**, 305810104 (2015).
- [52] E. Di Nezza, G. Palatucci, and E. Valdinoci, Hitchhiker’s guide to the fractional Sobolev spaces, *Bulletin des Sciences Mathématiques* **136**, 521 (2012).
- [53] C. Pozrikidis, *The Fractional Laplacian* (Chapman and Hall/CRC, New York, 2018).
- [54] A. Lischke, G. Pang, M. Gulian, F. Song, C. Glusa, X. Zheng, Z. Mao, W. Cai, M. M. Meerschaert, M. Ainsworth, *et al.*, What is the fractional Laplacian? a comparative review with new results, *Journal of Computational Physics* **404**, 109009 (2020).
- [55] J.-P. Bouchaud and A. Georges, Anomalous diffusion in disordered media: statistical mechanisms, models and physical applications, *Physics Reports* **195**, 127 (1990).
- [56] G. M. Zaslavsky, *Hamiltonian Chaos and Fractional Dynamics* (Oxford University Press, Oxford, 2005).
- [57] D. del-Castillo-Negrete, B. A. Carreras, and V. E. Lynch, Fractional diffusion in plasma turbulence, *Physics of Plasmas* **11**, 3854 (2004).
- [58] D. del-Castillo-Negrete, B. A. Carreras, and V. E. Lynch, Nondiffusive transport in plasma turbulence: A fractional diffusion approach, *Physical Review Letters* **94**, 065003 (2005).
- [59] D. del-Castillo-Negrete, Fractional diffusion models of nonlocal transport, *Physics of Plasmas* **13**, 082308 (2006).
- [60] R. Hilfer, *Applications of Fractional Calculus in Physics* (World Scientific, Singapore, 2000).
- [61] A. A. Schekochihin, J. T. Parker, E. G. Highcock, P. J. Dellar, W. Dorland, and G. W. Hammett, Phase mixing versus nonlinear advection in drift-kinetic plasma turbulence, *Journal of Plasma Physics* **82**, 905820212 (2016).
- [62] R. Gould, T. O’Neil, and J. Malmberg, Plasma wave echo, *Physical Review Letters* **19**, 219 (1967).
- [63] J. Malmberg, C. Wharton, R. Gould, and T. O’Neil, Plasma wave echo experiment, *Physical Review Letters* **20**, 95 (1968).
- [64] G. L. Eyink and J. Xin, Self-similar decay in the Kraich-

- nan model of a passive scalar, *Journal of Statistical Physics* **100**, 679 (2000).
- [65] G. K. Batchelor, Small-scale variation of convected quantities like temperature in turbulent fluid part 1. General discussion and the case of small conductivity, *Journal of Fluid Mechanics* **5**, 113 (1959).
- [66] This approximation may seem overly simplified; for example, it neglects collisions acting on $\langle f \rangle$, collisional drag, and nonlinearity [115]. However, we expect these effects to be subdominant compared to collisional diffusion of δf for the following reasons. In Section II A, we find that $\langle f \rangle$ satisfies a diffusion equation in velocity space. Its gradients therefore become ever smaller in time, so weak collisions will be negligible for $\langle f \rangle$. Collisional drag should be negligible in the limit $\nu \rightarrow 0^+$ because it contains one fewer velocity derivative than collisional diffusion. We assume that dropping nonlinearity in the collision operator is reasonable because we anticipate that δf will be small at the scales where collisions matter. Indeed, we find in Sections III and V that the Fourier spectrum of δf decays as a power law in wavenumber space, with collisional cutoffs occurring at large wavenumbers, where the spectrum is small relative to its magnitude at large scales.
- [67] K. Furutsu, *On the Statistical Theory of Electromagnetic Waves in a Fluctuating Medium (II)* (U.S. National Bureau of Standards, Washington, D.C., 1964).
- [68] E. A. Novikov, Functionals and the random-force method in turbulence theory, *Soviet Physics Journal of Experimental and Theoretical Physics* **20**, 1290 (1965).
- [69] A. Kolmogorov, The local structure of turbulence in incompressible viscous fluid at very large Reynolds numbers, *Doklady Akademii Nauk SSSR* **30**, 299 (1941).
- [70] P. Goldreich and S. Sridhar, Toward a theory of interstellar turbulence. 2. Strong Alfvénic turbulence, *Astrophysical Journal* **438**, 763 (1995).
- [71] A. A. Schekochihin, MHD turbulence: a biased review, *Journal of Plasma Physics* **88**, 155880501 (2022).
- [72] This solution can be directly compared to earlier results obtained in terms of the Hermite numbers m , as the Hermite transform is analogous to a Fourier transform when $m \gg 1$, with $m \sim s^2/2$ [35].
- [73] G. I. Barenblatt, *Scaling, self-similarity, and intermediate asymptotics* (Cambridge University Press, Cambridge, 1996).
- [74] M. Abramowitz and I. A. Stegun, *Handbook of Mathematical Functions with Formulas, Graphs, and Mathematical Tables* (Dover, New York, 1965).
- [75] A. Saichev and W. Woyczynski, *Distributions in the Physical and Engineering Sciences, Volume 1* (Birkhäuser, Boston, 1997).
- [76] The fact that the inertial-range spectrum (89) is scale-free and has no infrared cutoff means that v_{th} in (91) and (92) is formally an arbitrary velocity normalization for (89). However, to emphasize that the true spectrum has an outer scale at $sv_{\text{th}} \lesssim 1$, we still normalize s by v_{th} in (89).
- [77] For the source term to be non-zero, it is important that we do not take the limit $L_E \rightarrow \infty$, otherwise $\varepsilon \rightarrow 0$. This is because $\varepsilon \propto D_0^{-1/2} \propto L_E^{-\alpha/2}$, as can be seen in (39). Physically, turbulent diffusion is a large-scale effect and so is dominated by the largest electric-field scales. Note that any meaningful analysis of the spectrum in the case of $L_E \rightarrow \infty$ would require a time-dependent solution to (33) [64, 116, 117].
- [78] When $\alpha = 1$, (105) is proportional to a Hilbert transform [118] in k space. In plasma kinetics, non-local fluxes given by Hilbert transforms also show up in the context of Landau-fluid closures; viz., in the Hammett-Perkins closure [79], the heat flux is proportional to the Hilbert transform of the temperature (in position space).
- [79] G. W. Hammett and F. W. Perkins, Fluid moment models for Landau damping with application to the ion-temperature-gradient instability, *Physical Review Letters* **64**, 3019 (1990).
- [80] G. Hammett, W. Dorland, and F. Perkins, Fluid models of phase mixing, Landau damping, and nonlinear gyrokinetic dynamics, *Physics of Fluids B: Plasma Physics* **4**, 2052 (1992).
- [81] J. Podesta, J. Borovsky, and S. Gary, A kinetic Alfvén wave cascade subject to collisionless damping cannot reach electron scales in the solar wind at 1 AU, *The Astrophysical Journal* **712**, 685 (2010).
- [82] G. G. Howes, A prescription for the turbulent heating of astrophysical plasmas, *Monthly Notices of the Royal Astronomical Society: Letters* **409**, L104 (2010).
- [83] T. Passot and P. Sulem, A model for the non-universal power law of the solar wind sub-ion-scale magnetic spectrum, *The Astrophysical Journal Letters* **812**, L37 (2015).
- [84] M. Zhou, Z. Liu, and N. F. Loureiro, Electron heating in kinetic-Alfvén-wave turbulence, *Proceedings of the National Academy of Sciences* **120**, e2220927120 (2023).
- [85] To see this, consider the inertial-range equation for the spectrum (79). In the absence of nonlinearity, this equation is just $k \partial_s \hat{F} = 0$, whose solution is just $\hat{F} = \text{const.}$
- [86] C. Su and C. Oberman, Collisional damping of a plasma echo, *Physical Review Letters* **20**, 427 (1968).
- [87] Formally, this assumption is not valid in the Batchelor regime in the collisionless limit, since the total δC_2 stored in phase space and collision time τ_ν diverge, viz., (112). However, this divergence is only logarithmic, so one may expect quasi-steady states in the Batchelor regime to be possible when ν is finite.
- [88] J. T. Parker, E. G. Highcock, A. A. Schekochihin, and P. J. Dellar, Suppression of phase mixing in drift-kinetic plasma turbulence, *Physics of Plasmas* **23**, 070703 (2016).
- [89] R. Meyrand, A. Kanekar, W. Dorland, and A. A. Schekochihin, Fluidization of collisionless plasma turbulence, *Proceedings of the National Academy of Sciences* **116**, 1185 (2019).
- [90] L. D. Landau, On the vibrations of the electronic plasma, in *Collected Papers of L.D. Landau*, edited by D. ter Haar (Pergamon Press, Oxford, 1965) pp. 445–460.
- [91] J. M. TenBarge and G. Howes, Current sheets and collisionless damping in kinetic plasma turbulence, *Astrophysical Journal Letters* **771**, L27 (2013).
- [92] A. B. Navarro, B. Teaca, D. Told, D. Groselj, P. Crandall, and F. Jenko, Structure of plasma heating in gyrokinetic Alfvénic turbulence, *Physical Review Letters* **117**, 245101 (2016).
- [93] K. G. Klein, G. G. Howes, and J. M. TenBarge, Diagnosing collisionless energy transfer using field-particle

- correlations: gyrokinetic turbulence, *Journal of Plasma Physics* **83**, 535830401 (2017).
- [94] G. G. Howes, A. J. McCubbin, and K. G. Klein, Spatially localized particle energization by Landau damping in current sheets produced by strong Alfvén wave collisions, *Journal of Plasma Physics* **84**, 905840105 (2018).
- [95] J. Nättilä and A. M. Beloborodov, Heating of magnetically dominated plasma by Alfvén-wave turbulence, *Physical Review Letters* **128**, 075101 (2022).
- [96] C. Chen, K. Klein, and G. G. Howes, Evidence for electron Landau damping in space plasma turbulence, *Nature Communications* **10**, 1 (2019).
- [97] A. Afshari, G. Howes, C. Kletzing, D. Hartley, and S. Boardsen, The importance of electron Landau damping for the dissipation of turbulent energy in terrestrial magnetosheath plasma, *Journal of Geophysical Research: Space Physics* **126**, e2021JA029578 (2021).
- [98] M. M. Martinović, K. G. Klein, J. C. Kasper, A. W. Case, K. E. Korreck, D. Larson, R. Livì, M. Stevens, P. Whittlesey, B. D. Chandran, *et al.*, The enhancement of proton stochastic heating in the near-Sun solar wind, *Astrophysical Journal Supplement Series* **246**, 30 (2020).
- [99] D. Lynden-Bell, Statistical mechanics of violent relaxation in stellar systems, *Monthly Notices of the Royal Astronomical Society* **136**, 101 (1967).
- [100] B. Kadomtsev and O. Pogutse, Collisionless relaxation in systems with Coulomb interactions, *Physical Review Letters* **25**, 1155 (1970).
- [101] P.-H. Chavanis, Kinetic theory of collisionless relaxation for systems with long-range interactions, *Physica A: Statistical Mechanics and its Applications* **606**, 128089 (2022).
- [102] R. J. Ewart, A. Brown, T. Adkins, and A. A. Schekochihin, Collisionless relaxation of a Lynden-Bell plasma, *Journal of Plasma Physics* **88**, 925880501 (2022).
- [103] R. J. Ewart, M. L. Nastac, and A. A. Schekochihin, Non-thermal particle acceleration and power-law tails via relaxation to universal Lynden-Bell equilibria, *Journal of Plasma Physics* **89**, 905890516 (2023).
- [104] T. H. Dupree, Theory of phase space density granulation in plasma, *Physics of Fluids* **15**, 334 (1972).
- [105] E. Kawamori, Experimental verification of entropy cascade in two-dimensional electrostatic turbulence in magnetized plasma, *Physical Review Letters* **110**, 095001 (2013).
- [106] E. Kawamori and Y.-T. Lin, Evidence of entropy cascade in collisionless magnetized plasma turbulence, *Communications Physics* **5**, 338 (2022).
- [107] Z. Wu, J. He, D. Duan, X. Zhu, C. Hou, D. Verscharen, G. Nicolaou, C. J. Owen, A. Fedorov, and P. Louarn, Ion energization and thermalization in magnetic reconnection exhaust region in the solar wind, *The Astrophysical Journal* **951**, 98 (2023).
- [108] E. Godlewski and P.-A. Raviart, *Numerical approximation of hyperbolic systems of conservation laws* (Springer, New York, 1996).
- [109] G. Falkovich, Turbulence with an infinite number of conservation laws, *Physical Review E* **49**, 2468 (1994).
- [110] R. H. Kraichnan, Convection of a passive scalar by a quasi-uniform random straining field, *Journal of Fluid Mechanics* **64**, 737 (1974).
- [111] N. Aronszajn and K. T. Smith, Theory of Bessel potentials. I, *Annales de l'Institut Fourier* **11**, 385 (1961).
- [112] I. S. Gradshteyn and I. M. Ryzhik, *Table of Integrals, Series, and Products*, edited by D. Zwillinger and V. Moll (Elsevier, Amsterdam, 2014).
- [113] A. Kazantsev, Enhancement of a magnetic field by a conducting fluid, *Soviet Physics Journal of Experimental and Theoretical Physics* **26**, 1031 (1967).
- [114] F. Rincon, Dynamo theories, *Journal of Plasma Physics* **85**, 205850401 (2019).
- [115] P. Helander and D. J. Sigmar, *Collisional Transport in Magnetized Plasmas* (Cambridge University Press, Cambridge, 2005).
- [116] M. Chaves, G. Eyink, U. Frisch, and M. Vergassola, Universal decay of scalar turbulence, *Physical Review Letters* **86**, 2305 (2001).
- [117] M. Chertkov and V. Lebedev, Decay of scalar turbulence revisited, *Physical Review Letters* **90**, 034501 (2003).
- [118] F. W. King, *Hilbert Transforms*, Encyclopedia of Mathematics and its Applications, Vol. 1 (Cambridge University Press, 2009).